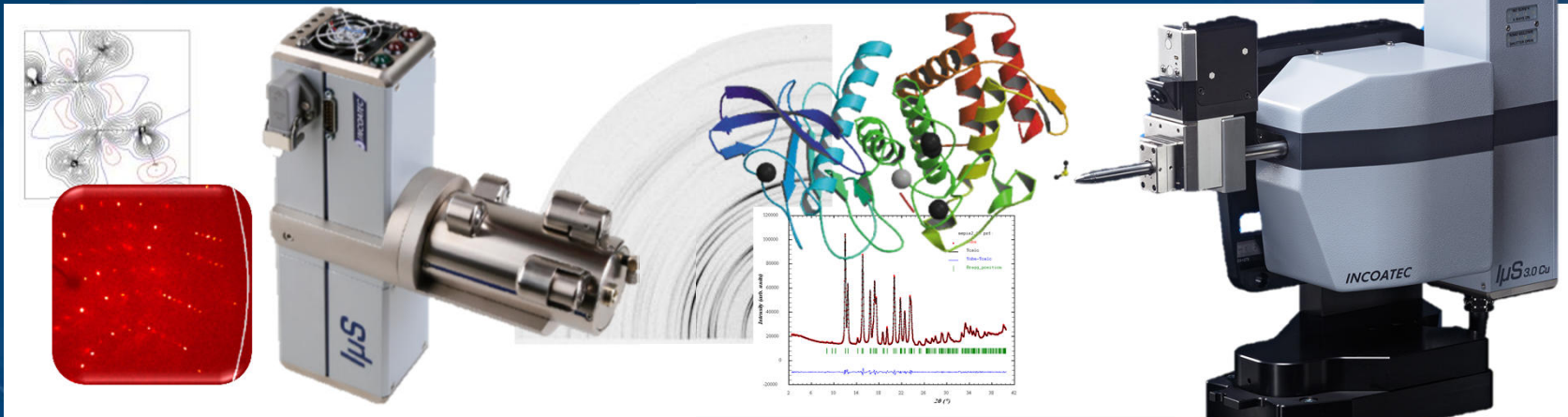




# The Incoatec Microfocus Source $\mu$ S

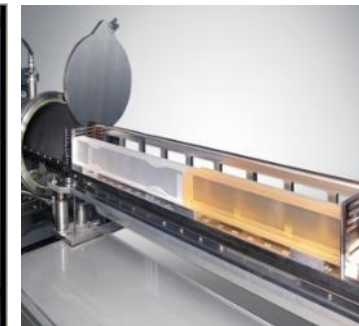
## 10 Years of $\mu$ S – A Retrospective



Jürgen Graf – Incoatec GmbH, Geesthacht, Germany

- Introduction
- What's new with the I $\mu$ S 3.0
- Microfocus Sources and Multilayer Mirrors – Technical Background
- Applications of the I $\mu$ S
  - Single Crystal Diffraction
  - Small Angle Scattering and General XRD

# Incoatec: Innovative Coating Technologies



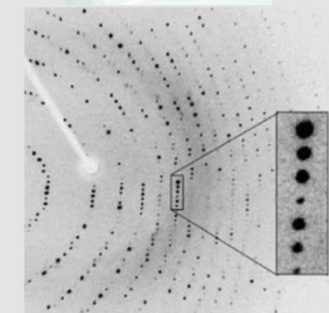
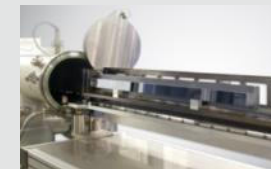
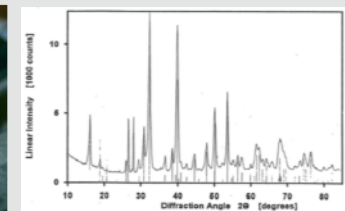
- Founded 2002 as **joint venture with Bruker AXS**, located in Geesthacht (near Hamburg)
- Production & development of **X-ray optics** and **microfocus X-ray sources**
- Equipment for **home-lab** instruments and **synchrotron** beamlines
- > 50 employees, new headquarter 4200 m<sup>2</sup>, > 10% invest for R&D



# Multilayers @ Incoatec

## A Brief History of Time

- 1989** Research on deposition and properties of thin films at GKSS research center
- 1993/94** Introduction of „Göbel-Mirrors“ by Herbert Göbel
- 1995** Joint development of Göbel mirrors in cooperation with Siemens
- 99 - 01** 1<sup>st</sup> synchrotron mirrors for FEL  
1<sup>st</sup> Montel Optics for SC-XRD
- 2002** Incoatec is incorporated as spin-off and joint venture with Bruker AXS
- 2006** Launch of the Cu- $\mu$ S ( $\mu$ S 1.0,
- 2015**  $\mu$ S 3.0 (AsCA Kolkatta)
- 2016** > 700  $\mu$ S's sold world wide

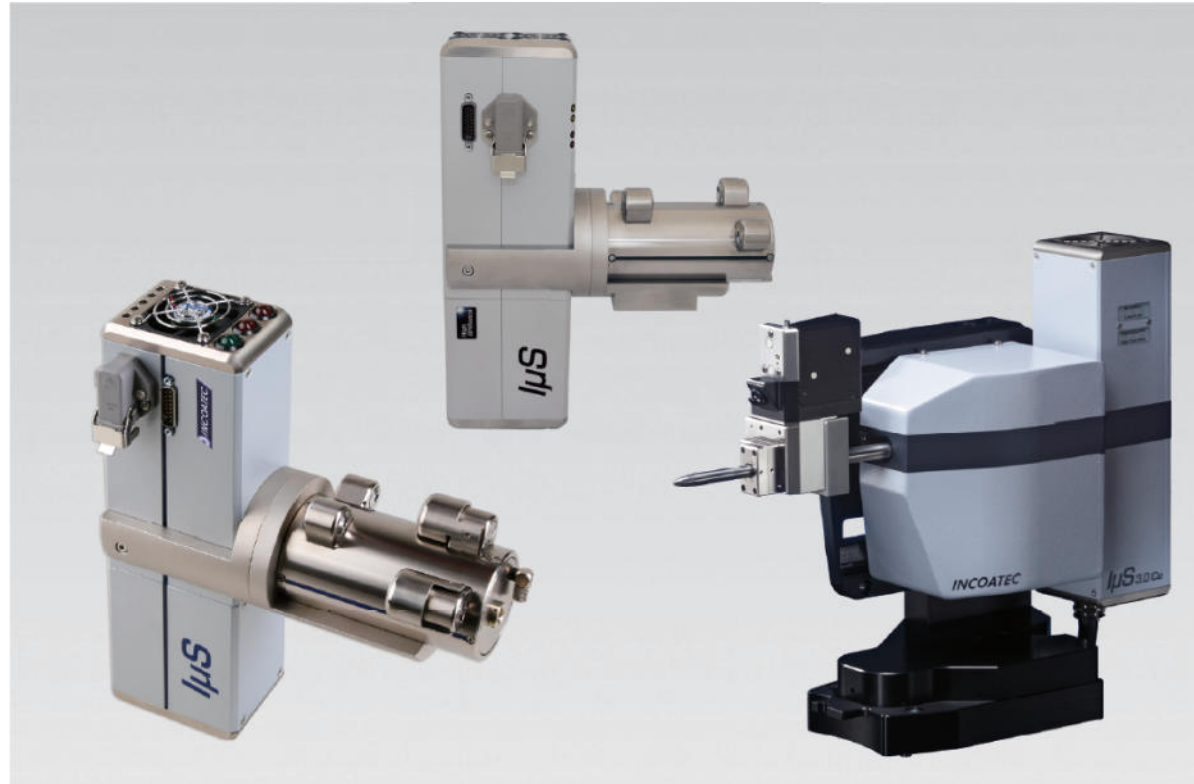


# The Incoatec Microfocus Source $\mu$ S



**Intensity Comparable to Traditional Rotating Anode Generators**

# 10 Years Incoatec Microfocus Source $\mu$ S



## ■ The $\mu$ S 3.0 – The Next Generation $\mu$ S

- **First and only** microfocus X-ray source designed for SC-XRD applications
- **New Tube:** Optimized tube parameters and improved heat management
- **New Beampath Concept:** Tube and optics are **pre-aligned** and **separately mounted** to an adapter plate for **true downstream alignment**
- **New “Quick-Lock”** mount for highly precise and reproducible mounting of source and optics
- **New Optics:** MX-3 mirror
- **More intensity without compromises in lifetime – always air-cooled !**



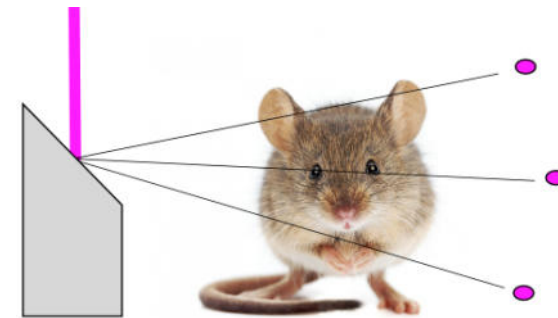
**30 – 40 % Intensity gain over  $\mu$ S HB**

# The $I\mu$ S 3.0 – The Next Generation $I\mu$ S

## Optimizing the $I\mu$ S 3.0 X-ray Tube

### ■ Conventional microfocus sealed tubes

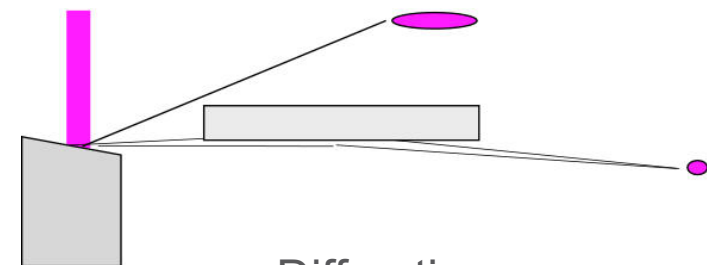
- Designed primarily for radiography (medical or NDT)
- **High take-off angles** and **smaller electron beam focus** in order to preserve resolution over a wide field of view



Radiography

### ■ The $I\mu$ S 3.0 tube:

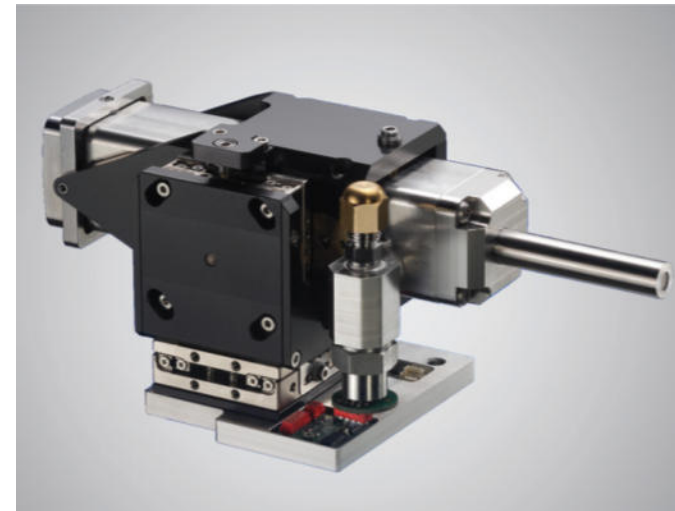
- Designed for X-ray diffraction
- No need for wide FOV and coherence
- **Reduced take-off angle** and **line-focused** e beam focus to match the view angle of the X-ray mirror
- **New filament** and **e beam optics**: more homogeneous and dense illumination



Diffraction

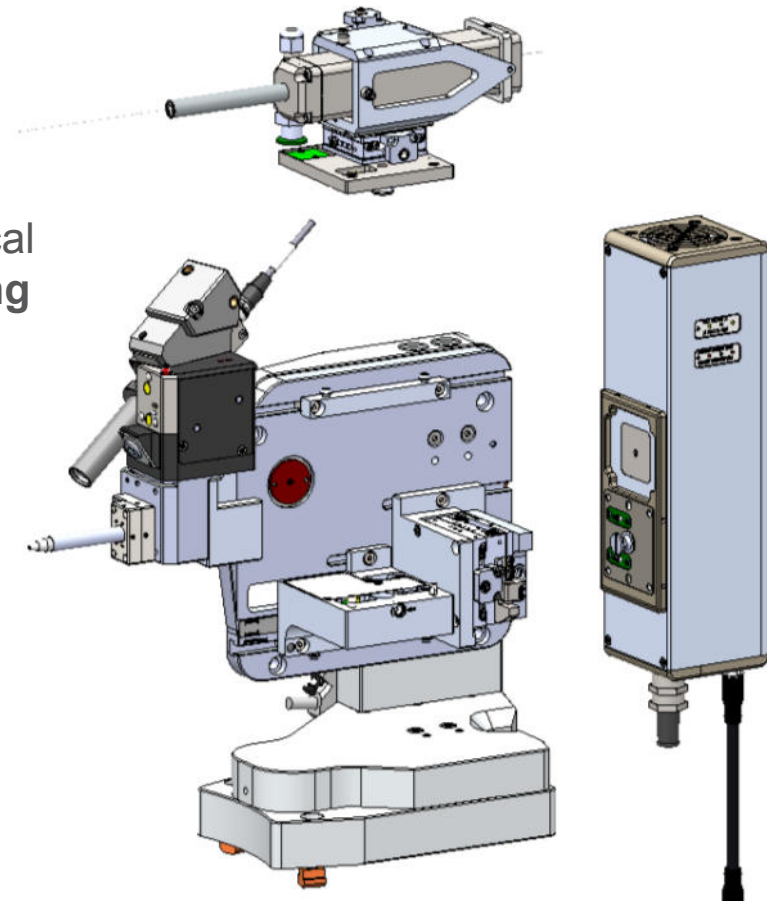
## ■ The Optics:

- New optics housing with **pre-set Bragg angle**
- Improved **X-ray optics** for Mo and Ag
- **New X-ray mirror** for Cu (**MX-3 optics**)
- **Encapsulated optics** housing filled with He
- He pressure ( $\sim 1.4$  bar) is monitored by a **pressure sensor**
- Less absorption due to **He flight tube**
- New „**Quick-Lock**“ mounting



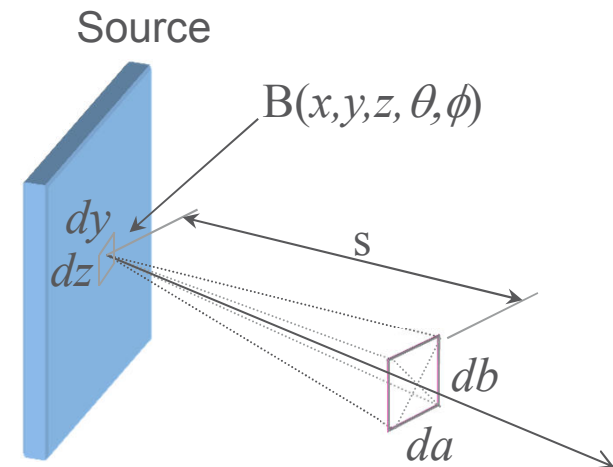
## ■ The Quick-Lock Concept:

- **Pre-aligned source and optics:**
  - both separately mounted on an optical bench **with just single screws using a well-defined torque** and high-precision mounts with pinning
  - **continuously adjustable** along the beam direction for precise setting of source-to-sample distance
- **Maximum intensity** on the sample
- Optics is **swappable** with a precision of below  $10\ \mu\text{m}$  at the sample position (!!!)
- **No instrument realignment** necessary after optics swap or tube change



## ■ Brilliance = Spectral Brightness B:

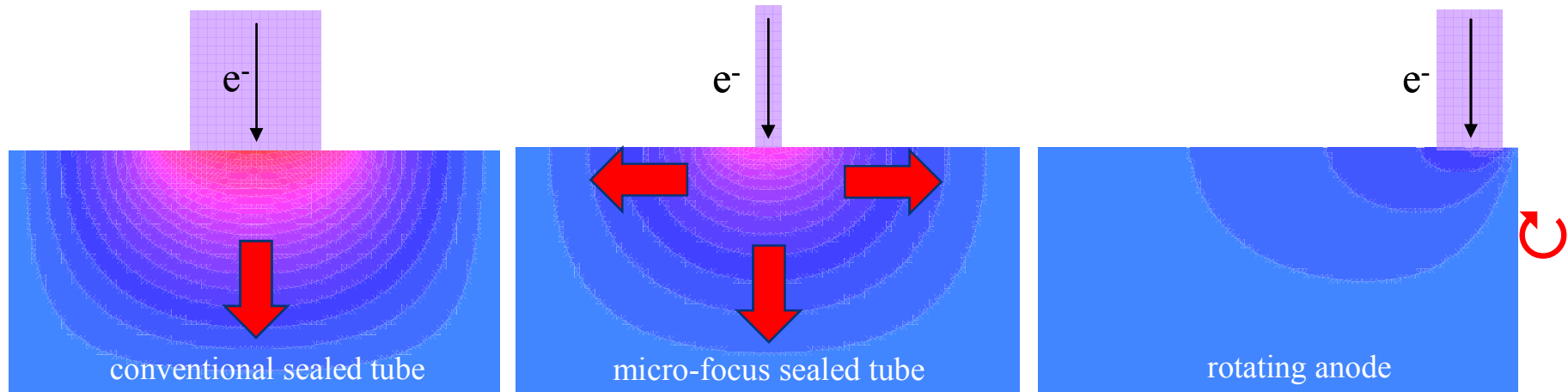
- is the number of photons in a given bandwidth emitted per unit time, per unit area and per unit solid angle
- B: [phts/s/mm<sup>2</sup>/mrad<sup>2</sup>/0.1% bandwidth]
- is a property of the source
- is proportional to the power load at the target and is, therefore, limited by the heat dissipation mechanism
- is a good measure for comparing sources



**High brightness means that the X-rays are highly “concentrated”.**

# Why Microfocus X-ray Sources?

## Power Load in All Solid-target X-ray Sources is Limited by Heat Dissipation



- Large Spot
- Quasi-1D heat flow limits power density
- $\sim 0.5 \text{ kW/mm}^2$

**Relative B: 1**

- Small Spot
- 2D heat flow allows more efficient cooling
- $\sim 5 \text{ kW/mm}^2$

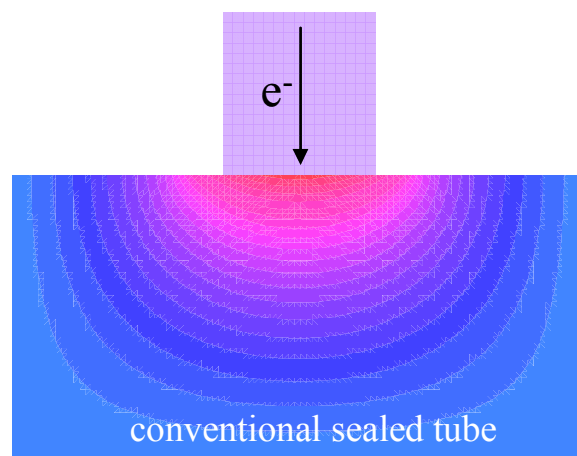
**Relative B:  $\sim 10$**

- Large or Small Spot
- Additional heat spread by rotation
- $> 15 \text{ kW/mm}^2$

**Relative B:  $> 10$**

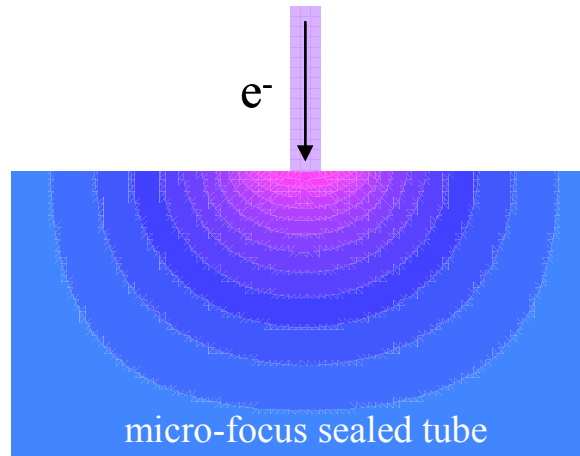
# Why Microfocus X-ray Sources?

## Power Load in All Solid-target X-ray Sources is Limited by Heat Dissipation



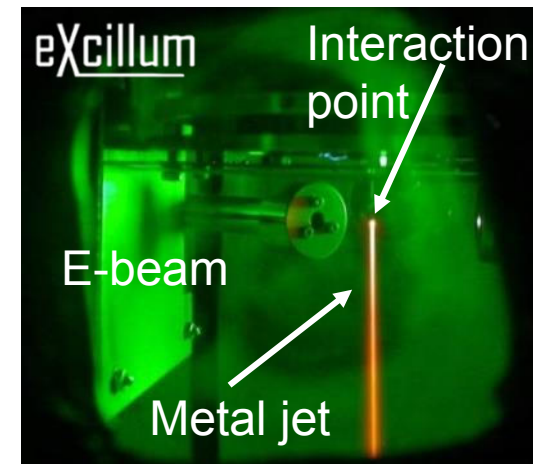
- Large Spot
- Quasi-1D heat flow limits power density
- $\sim 0.5 \text{ kW/mm}^2$

**Relative B: 1**



- Small Spot
- 2D heat flow allows more efficient cooling
- $\sim 5 \text{ kW/mm}^2$

**Relative B:  $\sim 10$**



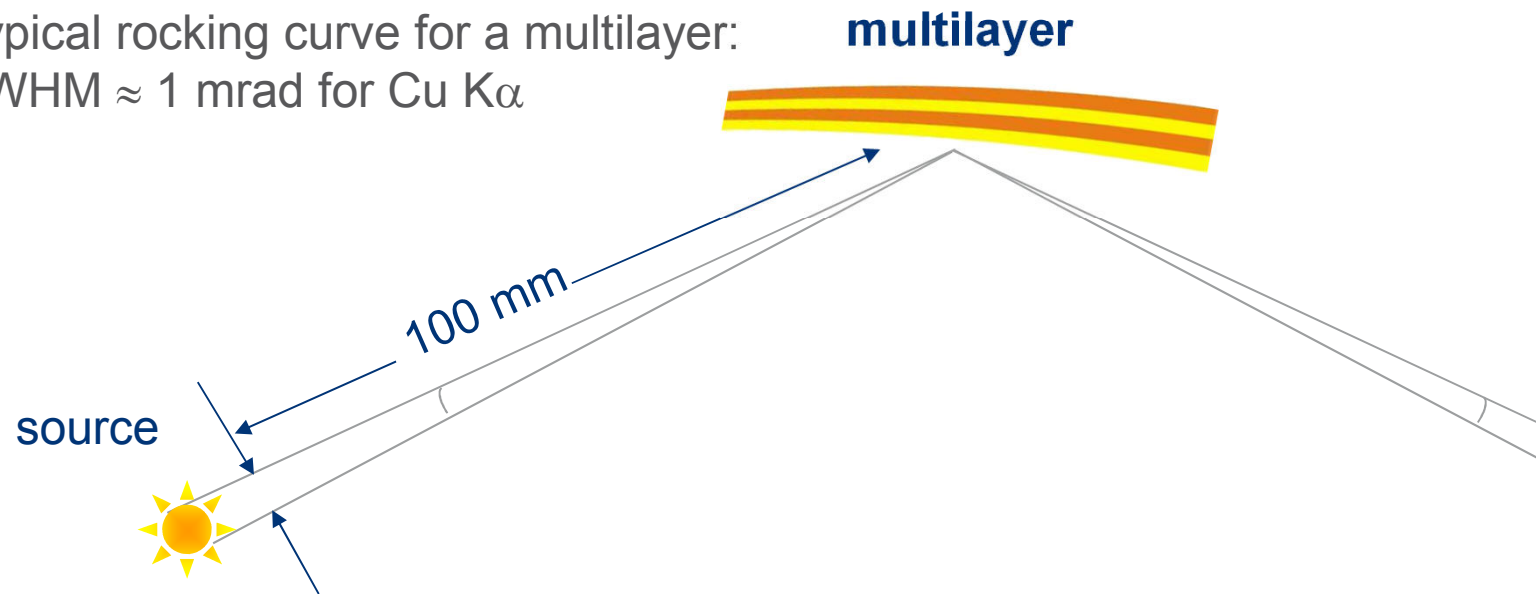
- Very small Spot
- High speed jet of liquid metal alloy
- $> 100 \text{ kW/mm}^2$

**Relative B:  $> 100$**

## Perfect Match: Multilayer Mirrors and Microfocus Sources

View angle = Bragg peak width

Typical rocking curve for a multilayer:  
FWHM  $\approx$  1 mrad for Cu  $K\alpha$

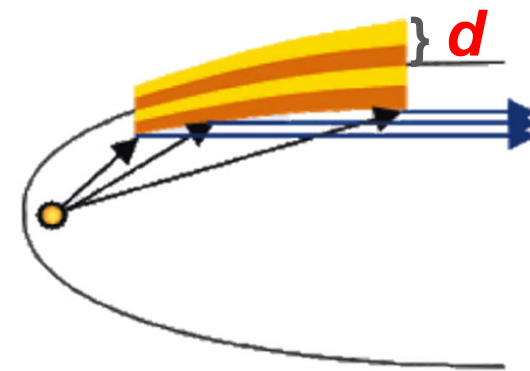


$$100 \text{ mm} * 1 \text{ mrad} = 100 \mu\text{m}$$

$$1 \text{ mrad} = 0.057 \text{ deg}$$

## ■ Multilayer Mirrors act as Bragg Reflector:

- collect as many photons as possible, select photons of a certain energy and redirect those to a sample by either focusing or collimating the X-ray beam
- alternating amorphous layers of a spacer (C, B<sub>4</sub>C, ...) and a reflector material (W, Ni, ...)
- following Bragg's law, the X-rays get reflected at the interfaces of the multilayer optics

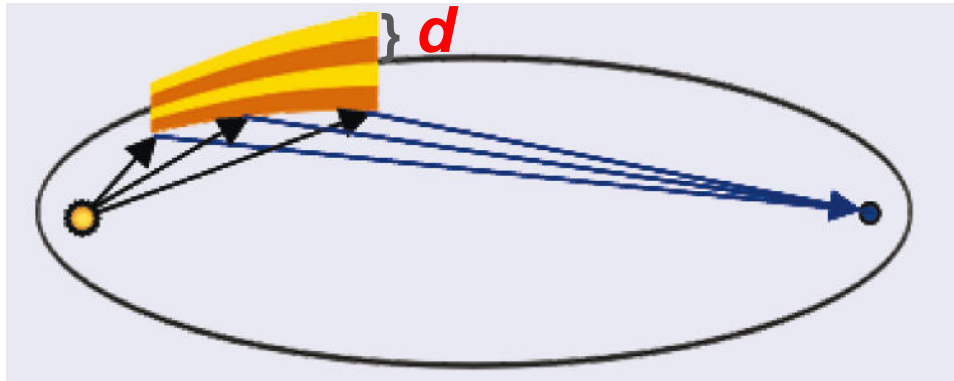


## ■ Advantages:

- High reflectivity and high spectral purity
- Flexible in design (*d*-spacing, divergence, beam size, ...)



## $d$ Spacing Gradient

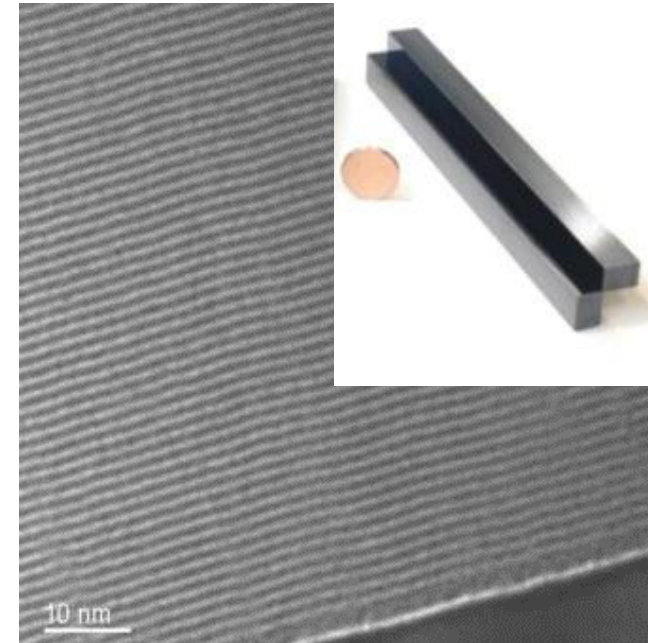


$$m \cdot \lambda = 2 \cdot d \cdot \sin \Theta$$

$$d = 2 - 6 \text{ nm}$$

$$\theta_m \approx 1.0^\circ \text{ (Cu-K}_\alpha\text{)}$$

$$\theta_m \approx 0.5^\circ \text{ (Mo-K}_\alpha\text{)}$$

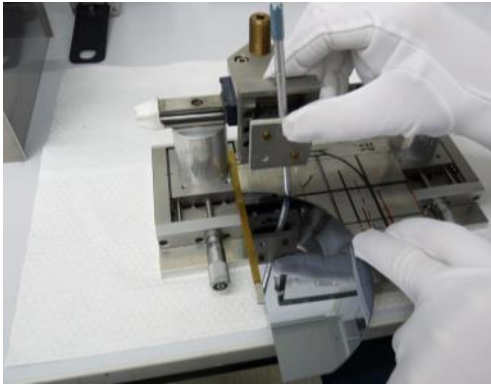


W/C Multilayer (TEM, Uni Kiel, Prof. Jäger)

~ 100 layer pairs

Tolerance in  $d$  spacing +/- 1%

# Manufacturing of a Multilayer X-ray Mirror



**Cutting of Si wafer**



**Bending of a substrate**



**2 „Fries“ (almost) ready for coating**



**Coating**

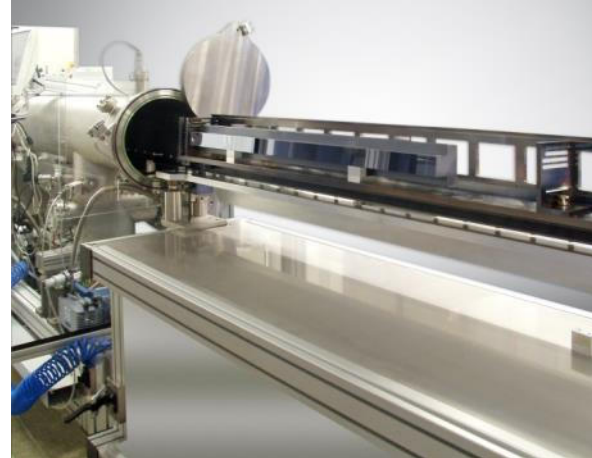


**Quality Control and Assembly**

# Magnetron Sputtering for Layer Deposition



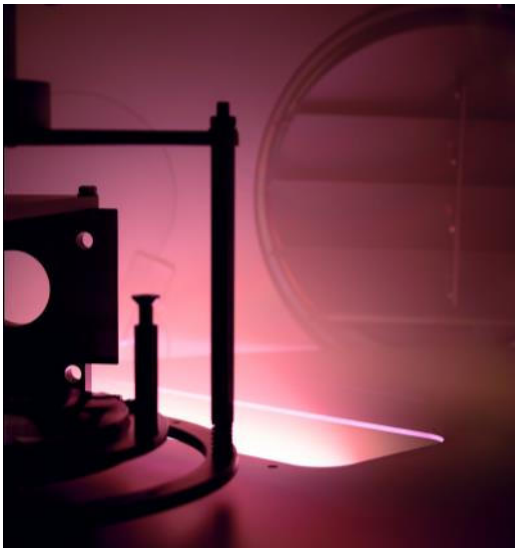
**Argon Plasma**



**Optimized Deposition Facilities for Different Sizes, Gradients and Precisions**

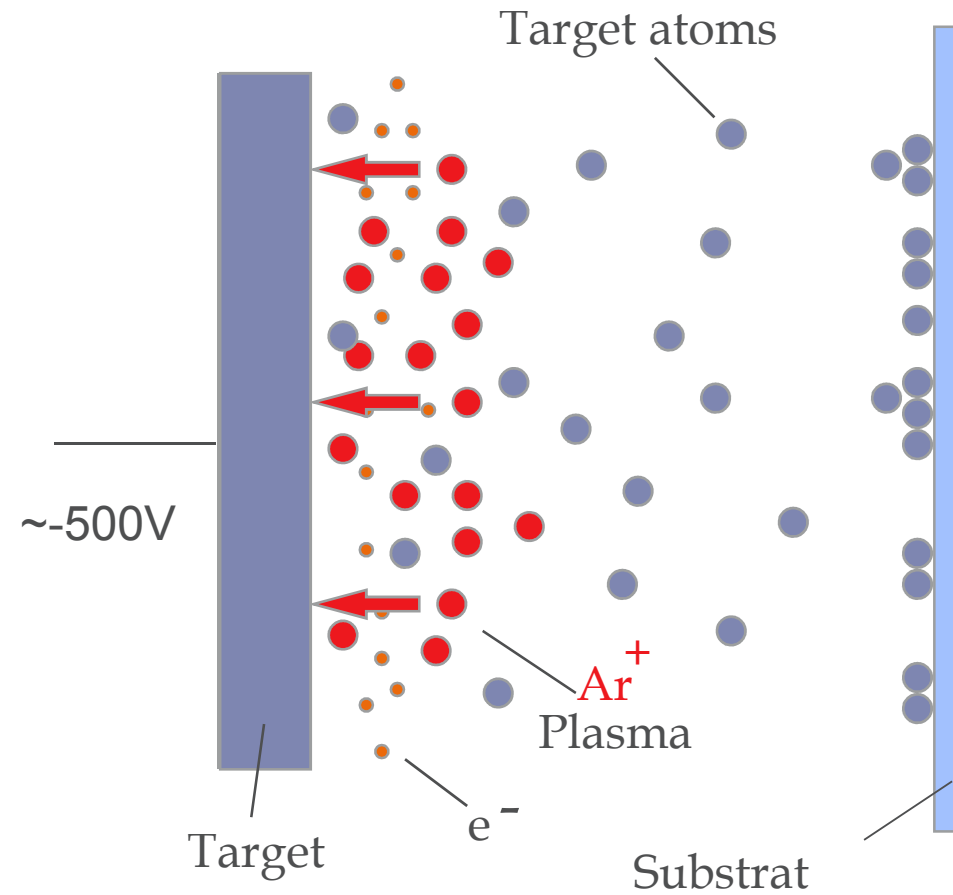
# Multilayer Deposition by Magnetron Sputtering

Vacuum <  $10^{-7}$  mbar  
Inert gas (Ar)  $10^{-3}$  mbar



## Requirements for high-quality multilayers:

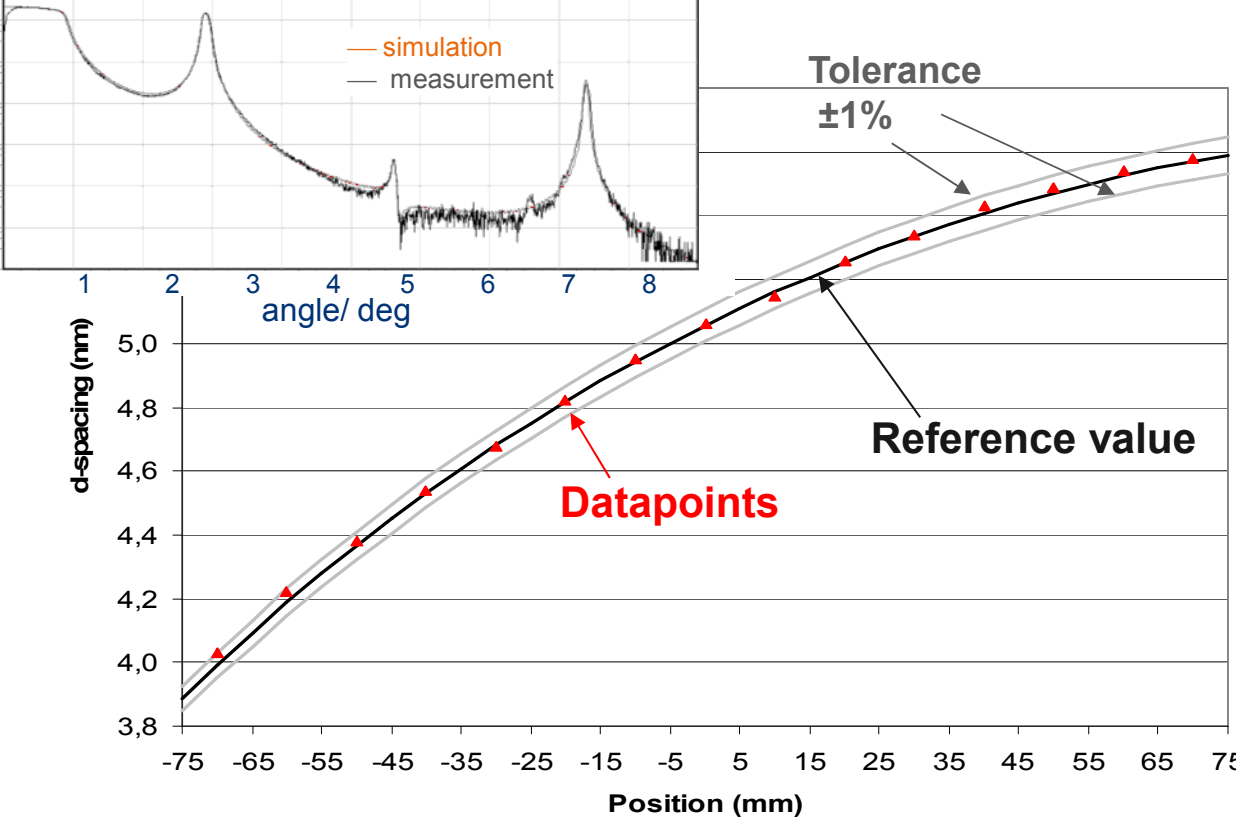
- well-defined interfaces
- reproducibility of the pairs



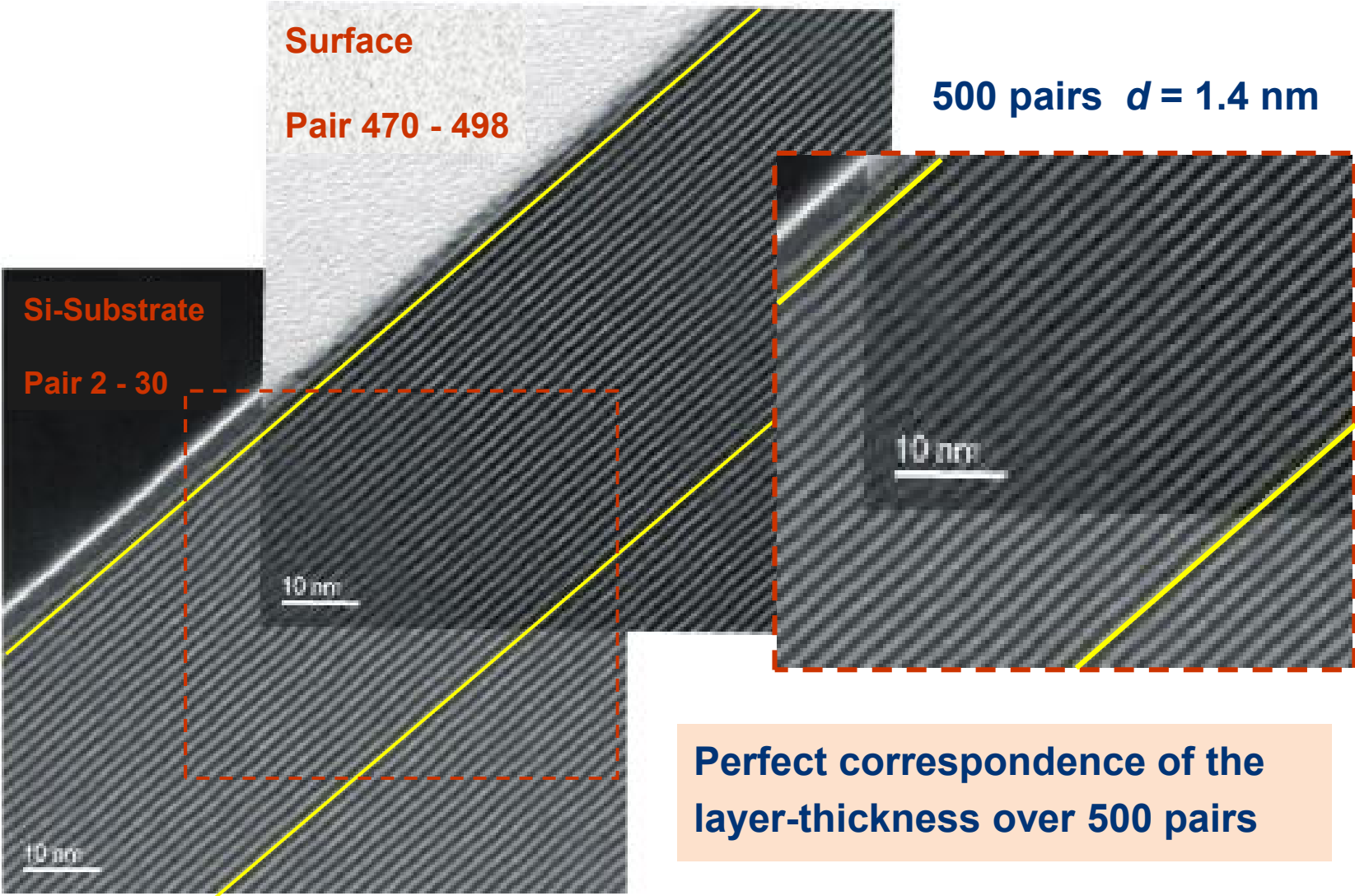
# X-ray Reflectometry for Characterization of Graded Multilayers



## Multilayer Optics for Crystallography in the Home-lab



# TEM-Picture of a Multilayer Coating

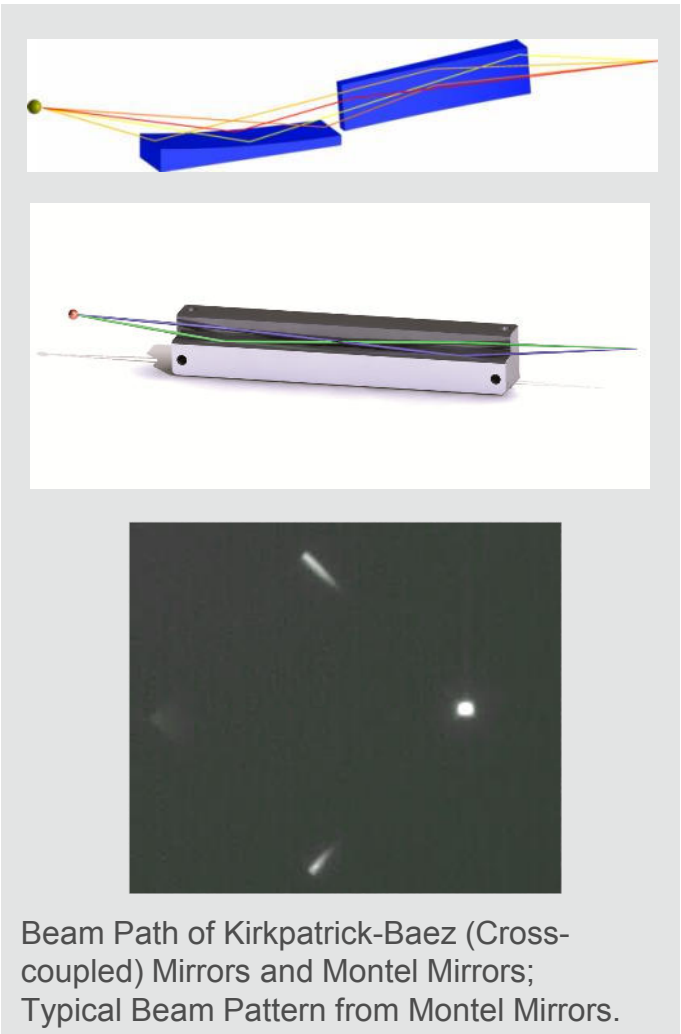


Perfect correspondence of the layer-thickness over 500 pairs

## Beam Profile of Montel Multilayer Mirrors

- **Modified Kirkpatrick-Baez Arrangement**
  - Two (identical) 1D bent mirrors in a side-by-side configuration
- **Benefits of the Montel Scheme**
  - More compact
  - Easy alignment
  - Symmetrical divergence spectrum

[www.x-ray-optics.de](http://www.x-ray-optics.de)



Beam Path of Kirkpatrick-Baez (Cross-coupled) Mirrors and Montel Mirrors;  
Typical Beam Pattern from Montel Mirrors.

# New Bruker AXS Instruments with one or two $\mu$ S's



D8 QUEST / VENTURE



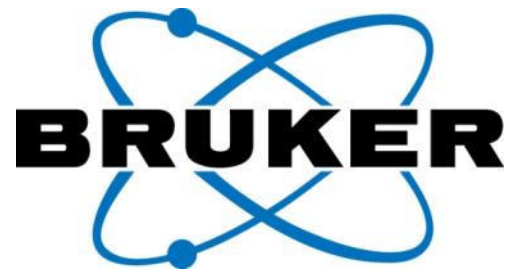
D8 ADVANCE / DISCOVER



D8 FABLINE

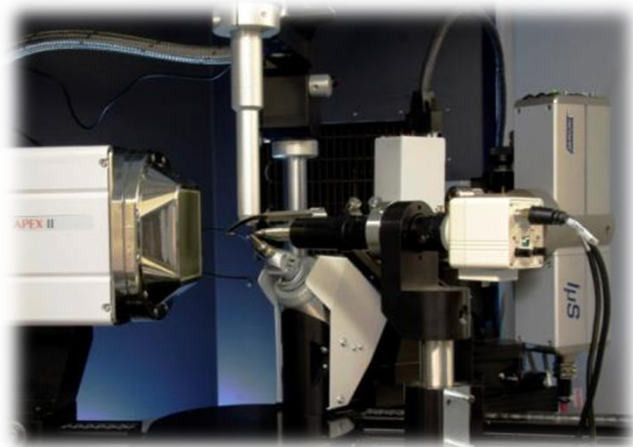


MICRO Series

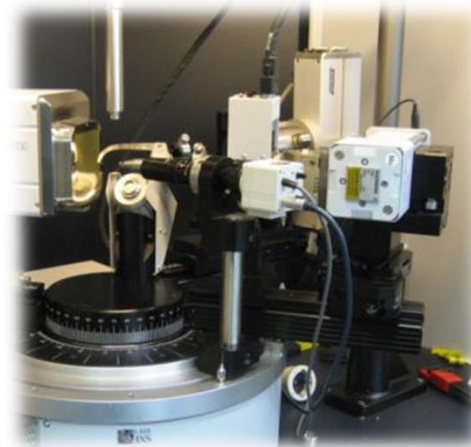


NANOSTAR

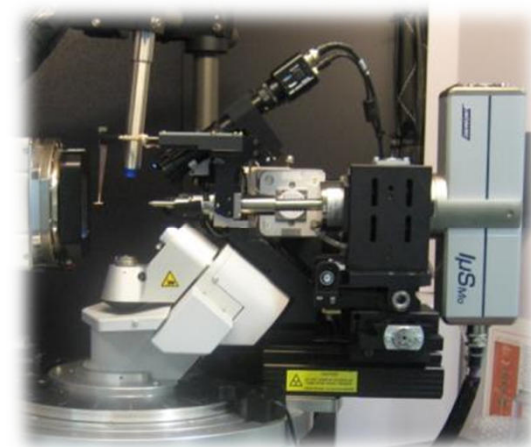
# $\mu$ S Upgrades on Bruker Instruments



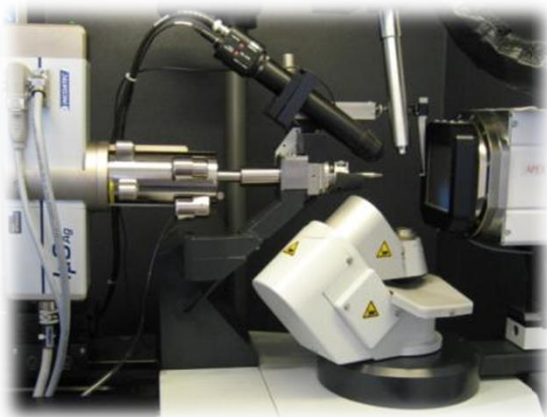
**SMART APEX II**



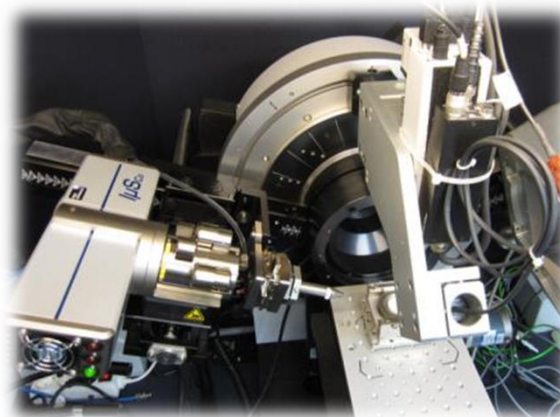
**SMART APEX as DUO**



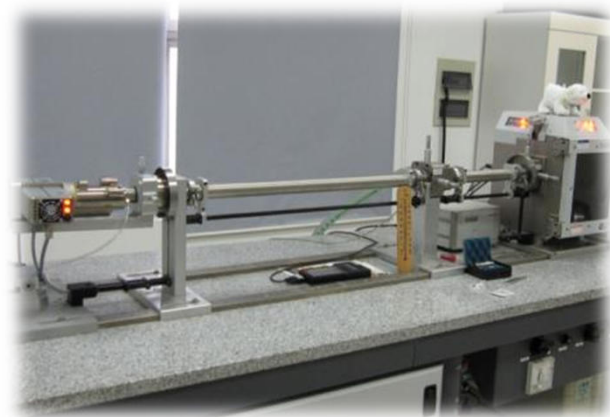
**KAPPA APEX II as DUO**



**X8 APEX / NONIUS KAPPA CCD**



**GADDS w/ VANTEC (XRD<sup>2</sup>)**



**NANOSTAR**

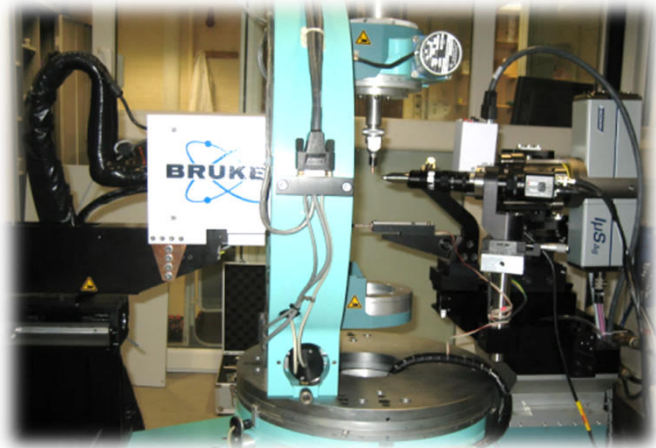
# $\mu$ S Upgrades on Other Vendor's Instruments



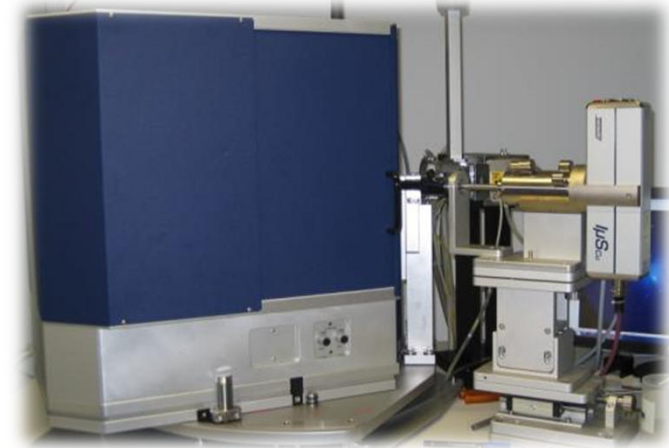
**marresearch mar345**



**Rigaku R-AXIS IV++**

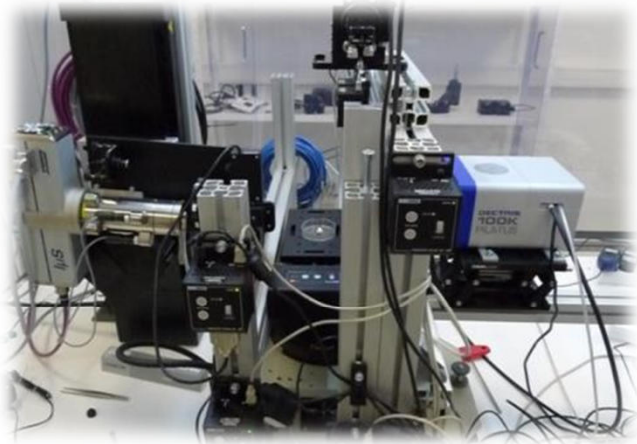


**Huber Eulerian Cradle**

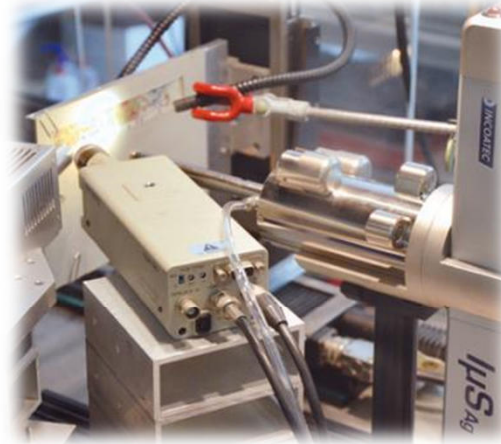


**STOE IPDS**

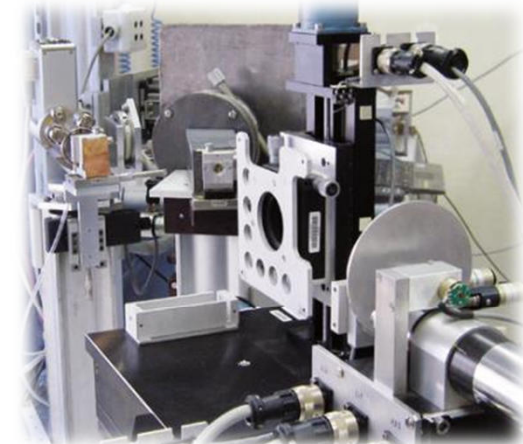
# $\mu$ S Upgrades on Customized Instruments



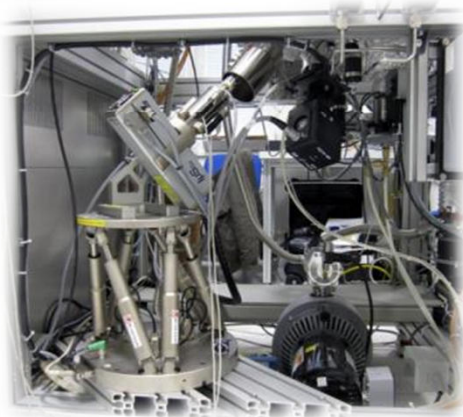
**(GI)SAXS w/ PILATUS**



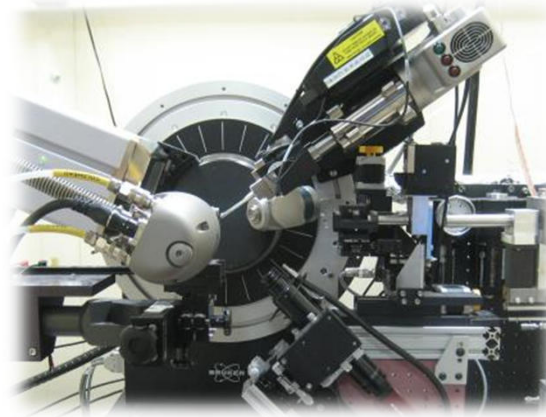
**XRD / XRF w/ PILATUS**



**XRD w/ Scintillation Counter**



**In-situ (GI)SAXS w/ PILATUS**



**SC-XRD Duo  $\mu$ S / Synchrotron**



**SAXS w/ marCCD**

## ■ The Incoatec X-ray Enclosure IXE

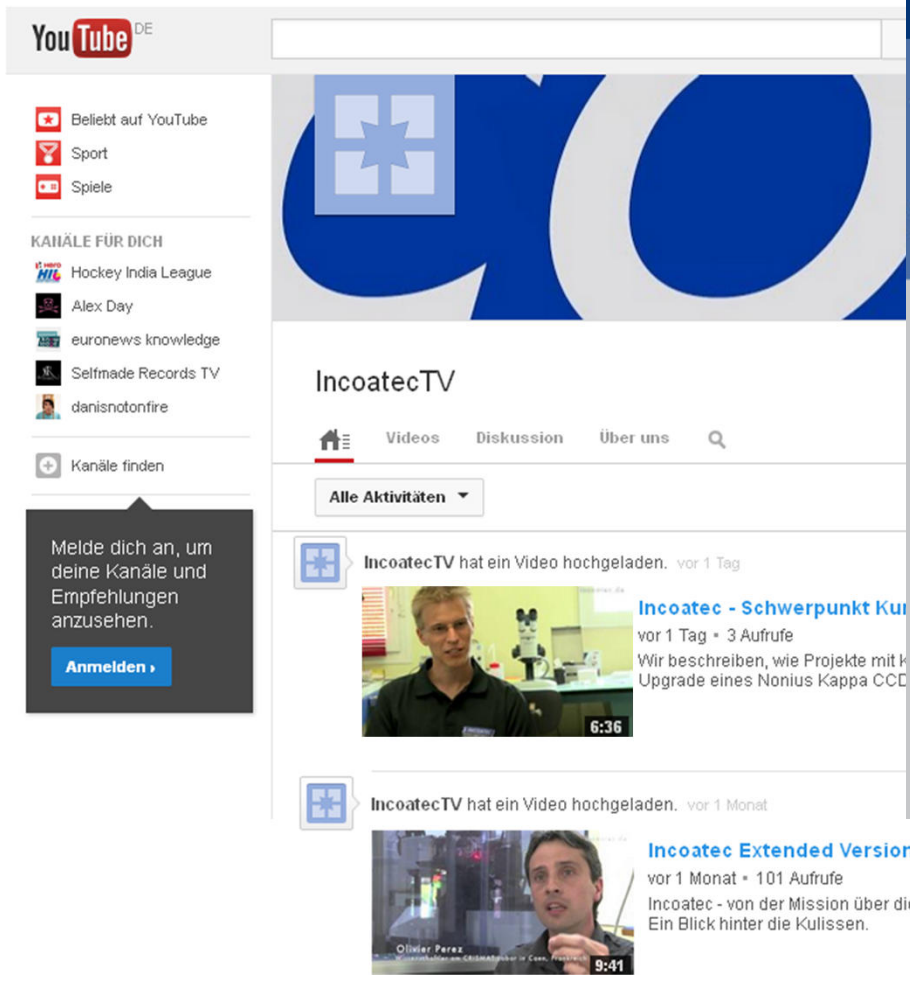
- Spacious cabinet for all common goniometers, detectors and dual wavelengths set-ups
- Guaranteed radiation safety for all  $1\mu\text{S}$  sources
- Compliant with the latest functional safety standards
- Tapped hole pattern plate for flexibility of experimental set-ups
- Removable panels for easy access
- Various radiation safe feedthroughs
- Dedicated space for a Dewar underneath the cabinet



**Solely Available with  $1\mu\text{S}$  and Stand-Alone HV Generator**

[www.youtube.com/user/IncoatecTV](http://www.youtube.com/user/IncoatecTV)

[www.incoatec.de/download](http://www.incoatec.de/download)



**IncoatecTV**

Videos Diskussion Über uns

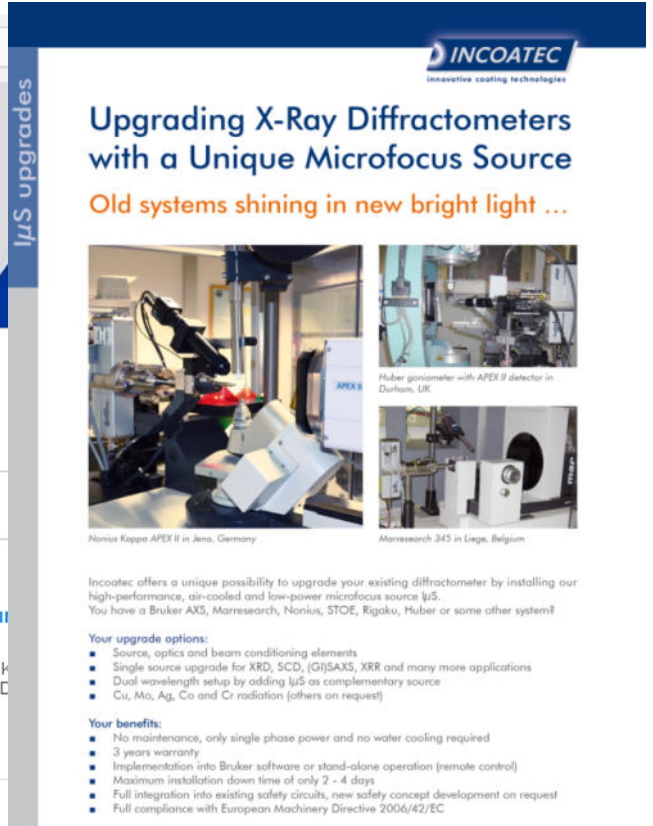
Alle Aktivitäten

IncoatecTV hat ein Video hochgeladen. vor 1 Tag

**Incoatec - Schwerpunkt Kunden**  
vor 1 Tag • 3 Aufrufe  
Wir beschreiben, wie Projekte mit der Upgrade eines Nonius Kappa CCD

IncoatecTV hat ein Video hochgeladen. vor 1 Monat

**Incoatec Extended Version - deutsch**  
vor 1 Monat • 101 Aufrufe  
Incoatec - von der Mission über die Optik- und Röhrenproduktion bis zur Kundeninstallation. Ein Blick hinter die Kulissen.



**INCOATEC**  
innovative coating technologies

**Upgrading X-Ray Diffractometers with a Unique Microfocus Source**  
Old systems shining in new bright light ...

Nonius Kappa APEX II in Jena, Germany  
Huber goniometer with APEX II detector in Durham, UK  
Marresearch 345 in Liege, Belgium

Incoatec offers a unique possibility to upgrade your existing diffractometer by installing our high-performance, air-cooled and low-power microfocus source  $\mu$ S.  
You have a Bruker AXS, Marresearch, Nonius, STOE, Rigaku, Huber or some other system?

**Your upgrade options:**

- Source, optics and beam conditioning elements
- Single source upgrade for XRD, SCD, (G)SAXS, XRR and many more applications
- Dual wavelength setup by adding  $\mu$ S as complementary source
- Cu, Mo, Ag, Co and Cr radiation (others on request)

**Your benefits:**

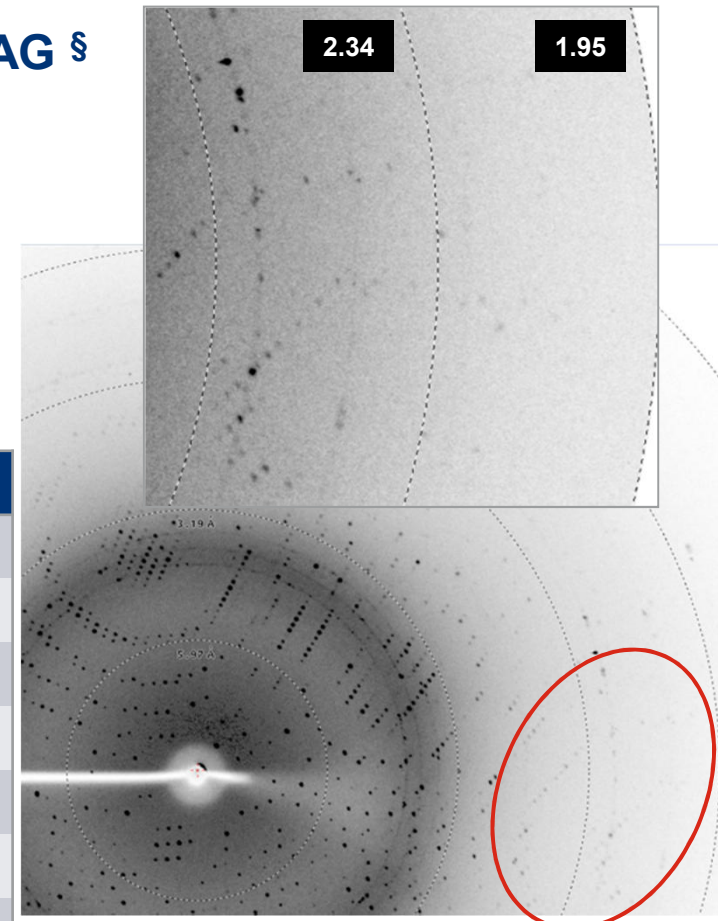
- No maintenance, only single phase power and no water cooling required
- 3 years warranty
- Implementation into Bruker software or stand-alone operation (remote control)
- Maximum installation down time of only 2 - 4 days
- Full integration into existing safety circuits, new safety concept development on request
- Full compliance with European Machinery Directive 2006/42/EC

## Very 1<sup>st</sup> Comparison of Cu- $\mu$ S vs. 4 kW Cu-RAG §

- Thermolysin Crystal (316 AA)
- Crystal Size: 0.20 x 0.06 x 0.04 mm<sup>3</sup>
- Space group:  $P6_122$
- Unit cell:  $a = b = 92.8 \text{ \AA}$ ,  $c = 130.0 \text{ \AA}$

Source	Cu- $\mu$ S	Rigaku RU 300
Detector	mar345	R-AXIS IV
Exposure time [min/°]	20	20
Resolution [ $\text{\AA}$ ]	<b>2.00</b> (2.03 - 2.00)	<b>2.10</b> (2.14-2.10)
$R$ (sym) [%]	<b>8.1</b> ( <b>46.7</b> )	<b>9.7</b> ( <b>45.1</b> )
$\langle I/\sigma \rangle$	<b>17.1</b> ( <b>3.2</b> )	<b>20.2</b> ( <b>4.4</b> )
Completeness [%]	97.9 (94.6)	99.9 (100)
Multiplicity	4.3 (4.5)	6.7 (6.6)

§ Rigaku RU 300 H3R, 1<sup>st</sup> generation multilayer mirror



Typical diffraction pattern of Thermolysin recorded with a Cu- $\mu$ S on a mardtb.

## Very 1<sup>st</sup> Comparison of Mo- $\mu$ S vs. 4 kW Mo-RAG §

Size [mm <sup>3</sup> ]	SiO <sub>2</sub>		CuSO <sub>4</sub>	
	0.04 x 0.04 x 0.02		0.07 x 0.05 x 0.05	
Source	Mo- $\mu$ S	FR 591	Mo- $\mu$ S	FR 591
Power [W]	30	4000	20	4000
Exposure time [s]	150 §	150 §	20 §	20 §
Normalized < I >	17.1	5.9	175.6	80.6
< $\sigma$ >	1.6	1.1	5.2	3.3
R1, wR2 [%]	8.4, 24.0	9.0, 24.1	3.5, 11.5	3.9, 12.2

§ Nonius FR591, flat graphite monochromator, 0.3 mm collimator, Nonius KappaCCD

## Very 1<sup>st</sup> Comparison of Mo- $\mu$ S vs. 4 kW Mo-RAG §

Size [mm <sup>3</sup> ]		CuSO <sub>4</sub>
Source		FR 591
Power [W]		4000
Exposure time [s]		20 §
Normalized < I >		80.6
< $\sigma$ >		3.3
R1, wR2 [%]		3.9, 12.2

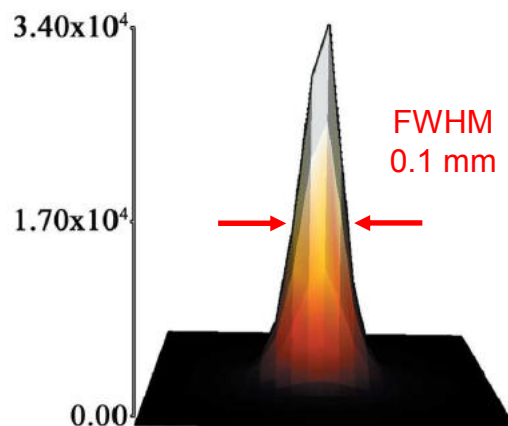
Size [mm <sup>3</sup> ]		0.07 x 0.05 x 0.05
Source		FR 591
Power [W]		4000
Exposure time [s]		20 §
Normalized < I >		80.6
< $\sigma$ >		3.3
R1, wR2 [%]		3.9, 12.2



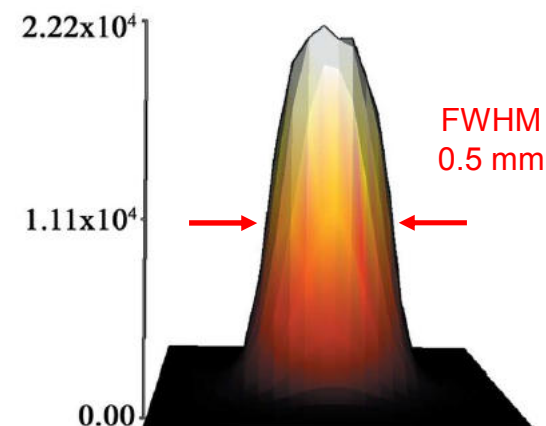
§ Nonius FR591, flat graphite monochromator, 0.3 mm collimator, Nonius KappaCCD

## Comparison of beam profiles from a focusing multilayer X-ray mirror and from a flat graphite monochromator

Multilayer Mirror

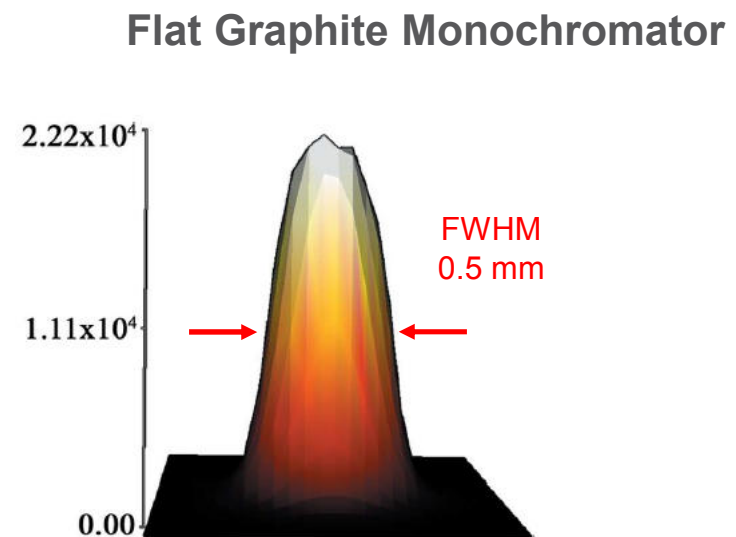
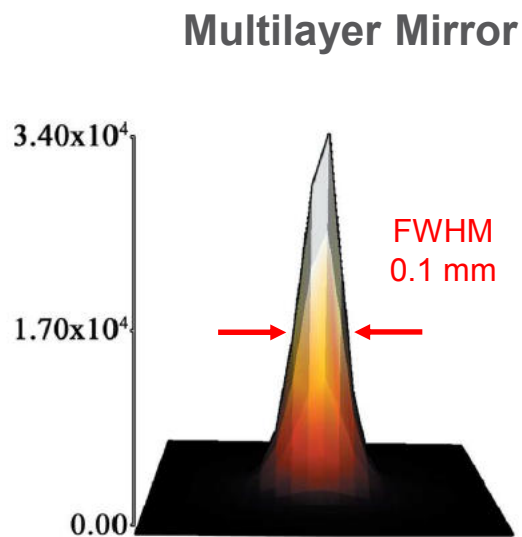


Flat Graphite Monochromator



- Symmetric Gaussian shaped beam
- Average FWHM:
  - Mo-I $\mu$ S: 0.110 mm
  - Ag-I $\mu$ S: 0.095 mm

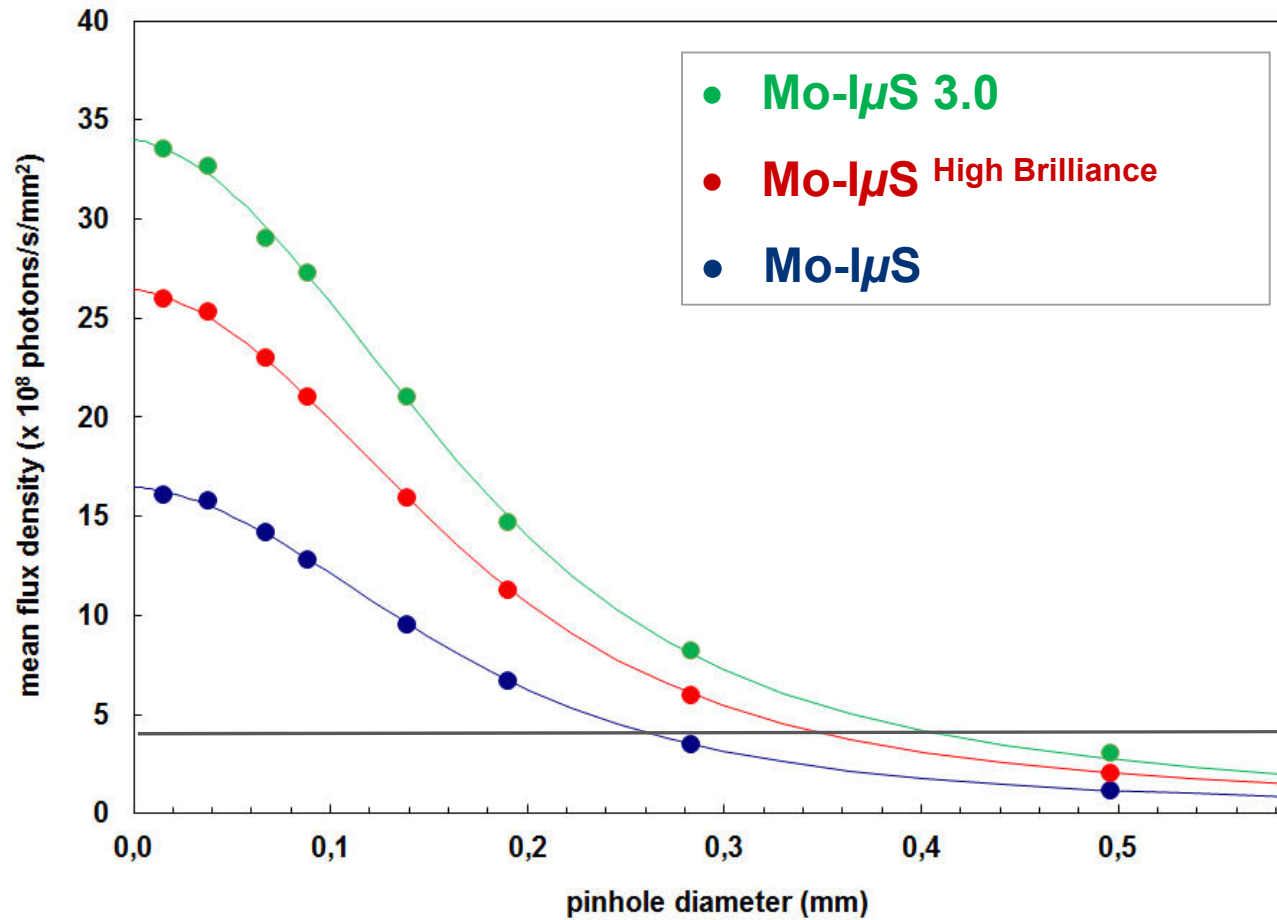
## Comparison of beam profiles from a focusing multilayer X-ray mirror and from a flat graphite monochromator



### Maximum Intensity on Small Diameter Ideal small crystals (in air or gasket)

- Mo-I $\mu$ S: 0.110 mm
- Ag-I $\mu$ S: 0.095 mm

## Flux through pinholes w/ different diameter (calibrated PN diode)

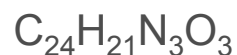


2 kW Mo ST

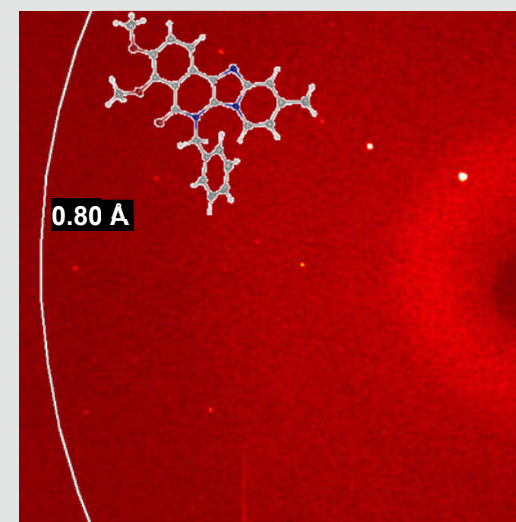
# Comparison 2 kW Mo ST vs. Mo- $\mu$ S

## Data from Small Crystal of Organic Compound

Size [mm <sup>3</sup> ]	0.10 x 0.05 x 0.05	
Source	Mo ST	Mo- $\mu$ S
Power [W]	2000	30
Exposure time	90 s/0.3°	<b>30 s/0.3°</b>
Resolution [Å]	<b>0.75</b> (0.85 – 0.75)	<b>0.75</b> (0.85 – 0.75)
Normalized < I > *	<b>19</b>	<b>139</b>
< I/σ >	<b>10.7 (2.1)</b>	<b>15.3 (3.5)</b>
R1, wR2 [%]	5.55, 10.44	3.88; 9.16
Distance N – C [Å]	<b>1.325(4)</b>	<b>1.325(3)</b>



\* Normalized to 1 °/min

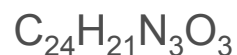


Typical diffraction pattern ( $P2_1$ ,  
 $a = 8.3628(6)$  Å,  $b = 7.0469(5)$  Å,  
 $c = 15.9737(11)$  Å,  $\beta = 92.210(1)^\circ$ ,  $Z = 2$ )

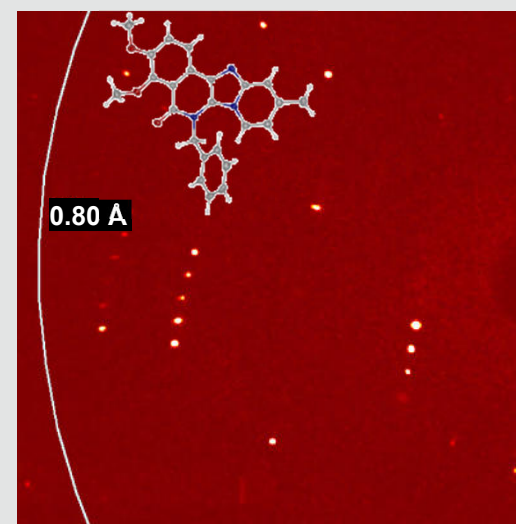
# Comparison 2 kW Mo ST vs. Mo- $\mu$ S

## Data from Larger Crystal of Organic Compound

Size [mm <sup>3</sup> ]	0.30 x 0.25 x 0.15	
Source	Mo ST	Mo- $\mu$ S
Power [W]	2000	30
Exposure time	15 s/0.3°	10 s/0.3°
Resolution [Å]	0.75 (0.85 – 0.75)	0.75 (0.85 – 0.75)
Normalized $\langle I \rangle^*$	1286	4763
$\langle I/\sigma \rangle$	30.4 (13.6)	37.6 (21.1)
R1, wR2 [%]	3.17, 8.16	3.08; 8.18
Distance N – C [Å]	1.324(2)	1.323(2)



\* Normalized to 1 °/min



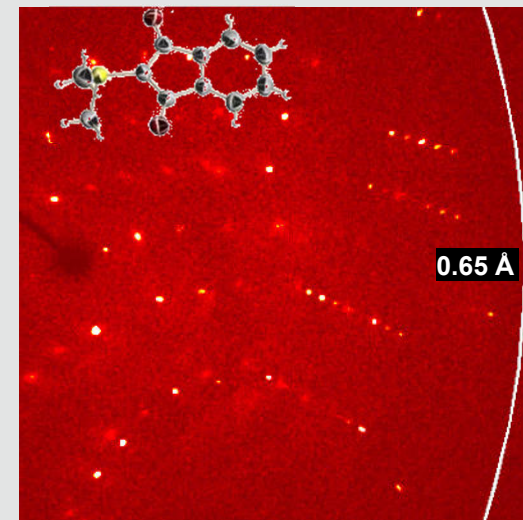
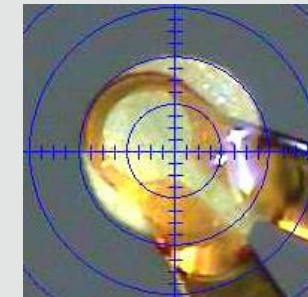
Typical diffraction pattern ( $P2_1$ ,  
 $a = 8.3628(6)$  Å,  $b = 7.0469(5)$  Å,  
 $c = 15.9737(11)$  Å,  $\beta = 92.210(1)^\circ$ ,  $Z = 2$ )

# Comparison 2 kW Mo ST vs. Mo- $\mu$ S HB

## Ylid Data from 2 kW Mo ST vs. Mo- $\mu$ S HB

Size [mm <sup>3</sup> ]	0.40 x 0.40 x 0.40	
Source	Mo ST	Mo- $\mu$ S HB
Power [W]	2000	50
Exposure time	20 s/°, 4 h	20 s/°, 4 h
Resolution [Å]	<b>0.65</b> (0.75 – 0.65)	<b>0.65</b> (0.75 – 0.65)
Normalized $\langle I \rangle$	<b>2252.7</b>	<b>12285.4</b>
$\langle I/\sigma \rangle$	<b>27.9 (7.1)</b>	<b>46.6 (17.3)</b>
R1, wR2 [%]	3.36, 9.02	2.97; 8.37
Flack $x(u)$	<b>0.02(3)</b>	<b>0.04(1)</b>
Distance C – C [Å]	<b>1.398(3)</b>	<b>1.399(2)</b>

**Better Data despite the fact that Crystal is Larger than the Beam**

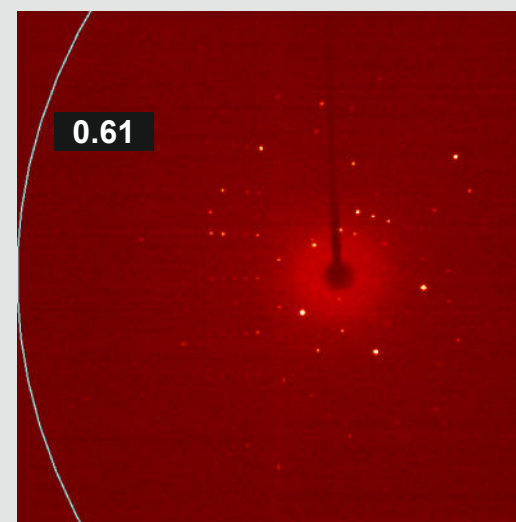
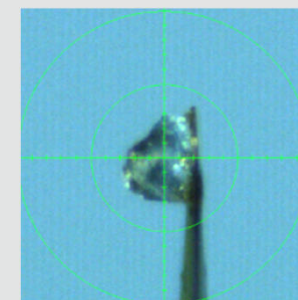


Typical diffraction pattern ( $P2_12_12_1$ ,  
 $a = 5.9598(2)$  Å,  $b = 9.0361(2)$  Å,  
 $c = 18.3870(5)$  Å,  $Z = 4$ )

## Real Life Example: Diphenyloxazolidin-2-one Derivate

Source	Mo- $\mu$ S HB	Mo- $\mu$ S 3.0
Detector	PHOTON100	PHOTON100
Exposure time	35 s/0.3°, 15 h	35 s/0.3°, 15 h
Resolution [Å]	0.64 (0.74 – 0.64)	0.61 (0.71 – 0.61)
Multiplicity	9.3 (4.5)	8.4 (2.8)
$\langle I/\sigma \rangle$	23.0 (3.1)	27.5 (3.4)
R1, wR2 [%]	7.17, 14.77	6.53, 14.36
d(C-C) [Å]	1.387(4)	1.390(3)
Parsons z(v)	0.0(3)	0.1(2)

$C_{25}H_{31}NO_5$ , 0.12 x 0.10 x 0.09 mm<sup>3</sup>,  
comparable strategies



Typical diffraction pattern ( $P2_12_12_1$ ,  
 $a = 8.4394(2)$  Å,  $b = 13.7322(4)$  Å,  
 $c = 19.3182(6)$  Å,  $Z = 4$ )

## Comparison of Different Instrument Generations with a Real Life Crystal

- Comparison of data from same purely organic crystal, collected at 100 K with Mo-K $\alpha$  radiation and comparable data collection strategies



**APEX II QUAZAR:**

Mo-I $\mu$ S w/ APEX II



**D8 VENTURE:**

Mo-I $\mu$ S HB w/ PHOTON100



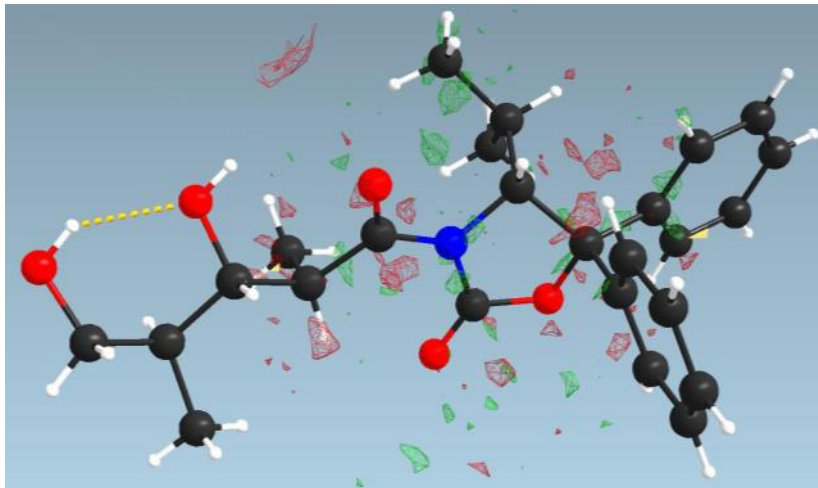
**D8 VENTURE 2<sup>nd</sup> Gen.:**

Mo-I $\mu$ S 3.0 w/ PHOTON II

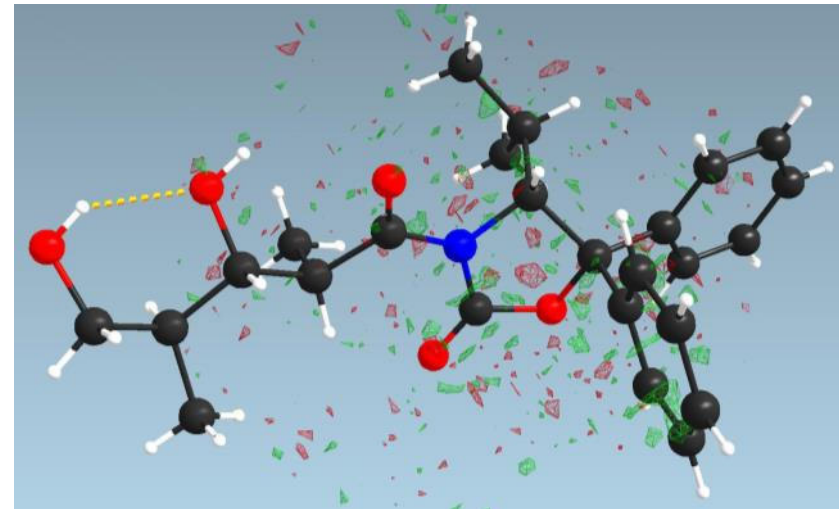
## Diphenyloxazolidin-2-one Derivate: Increased Depth of Information

Source	Mo-I $\mu$ S	Mo-I $\mu$ S HB	Mo-I $\mu$ S 3.0
Detector	APEX II	PHOTON100	PHOTON II
Exposure time	20 s/0.3°, <b>17 h</b>	35 s/0.3°, <b>15 h</b>	35 s/0.3°, <b>15 h</b>
Max. Res. [Å]	0.73	0.64	<b>&lt; 0.56</b>
Resolution [Å]	0.80 (0.90 – 0.80)	0.80 (0.90 – 0.80)	0.80 (0.90 – 0.80)
Multiplicity	10.1 (8.4)	12.7 (9.1)	11.7 (9.3)
<I/ $\sigma$ >	32.0 ( <b>4.8</b> )	41.6 ( <b>9.7</b> )	<b>55.2 (18.8)</b>
R1(all), wR2(all) [%]	4.24, 11.48	7.17, 14.77	8.11, 18.43
d(C-C) [Å]	1.384(4)	1.387(4)	1.390( <b>3</b> )
Parsons z( $\nu$ )	0.0( <b>4</b> )	0.0( <b>3</b> )	0.1( <b>2</b> )
Highest peak [eÅ <sup>-3</sup> ]	0.14	0.36	0.63

## Real Life Example: Diphenyloxazolidin-2-one Derivate: Residual Densities

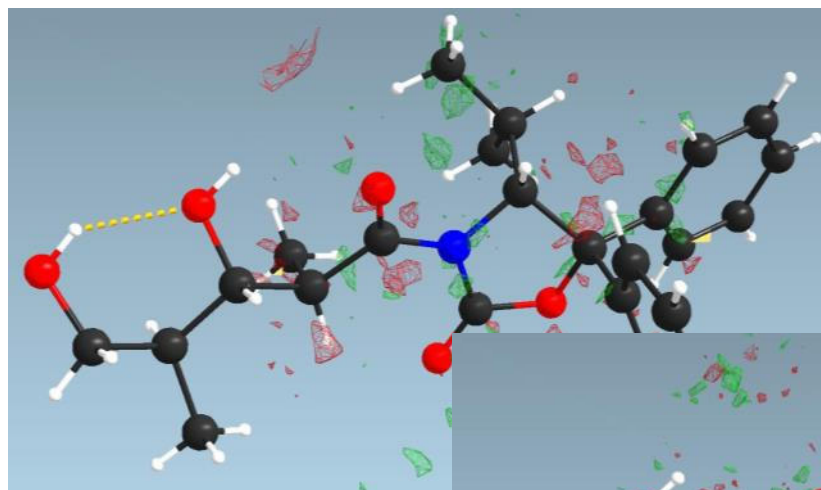


Mo- $I\mu$ S plus APEX II, max.  
resolution 0.73 Å,  $\pm 0.08$  e/Å<sup>3</sup>

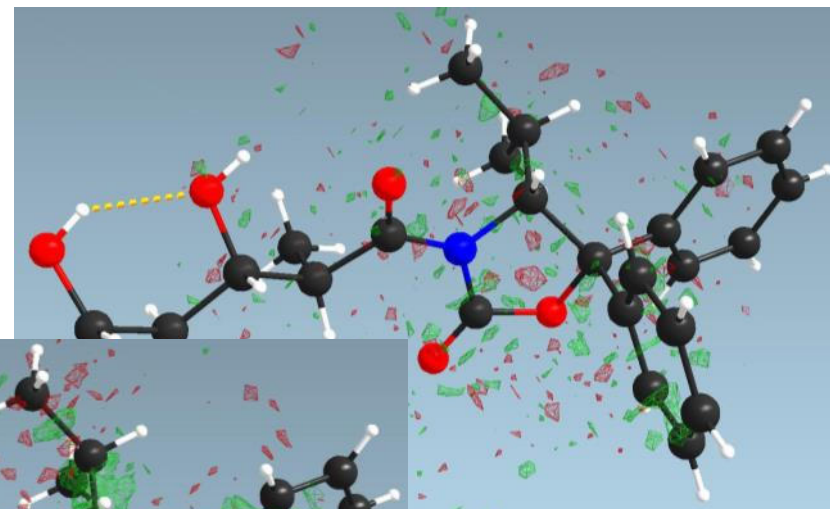


Mo- $I\mu$ S HB plus PHOTON100,  
max. resolution 0.64 Å,  $\pm 0.25$  e/Å<sup>3</sup>

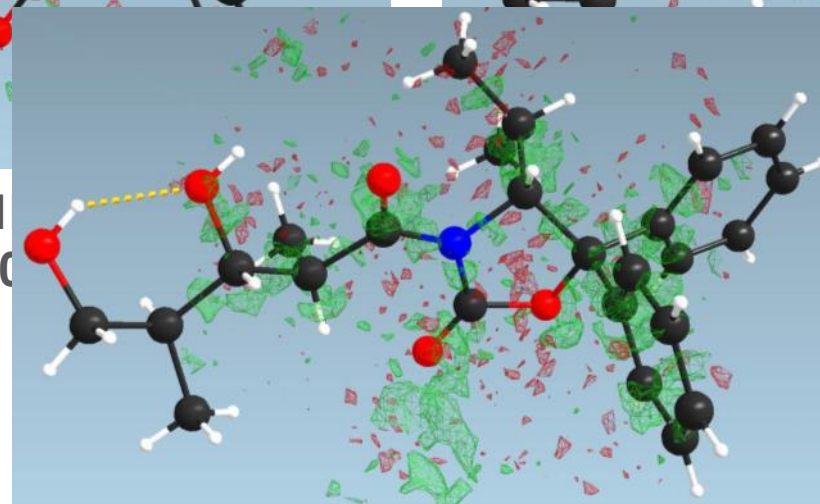
## Real Life Example: Diphenyloxazolidin-2-one Derivate: Residual Densities



Mo-I $\mu$ S plus APEX I  
resolution 0.73 Å,  $\pm 0.25$  e/Å<sup>3</sup>

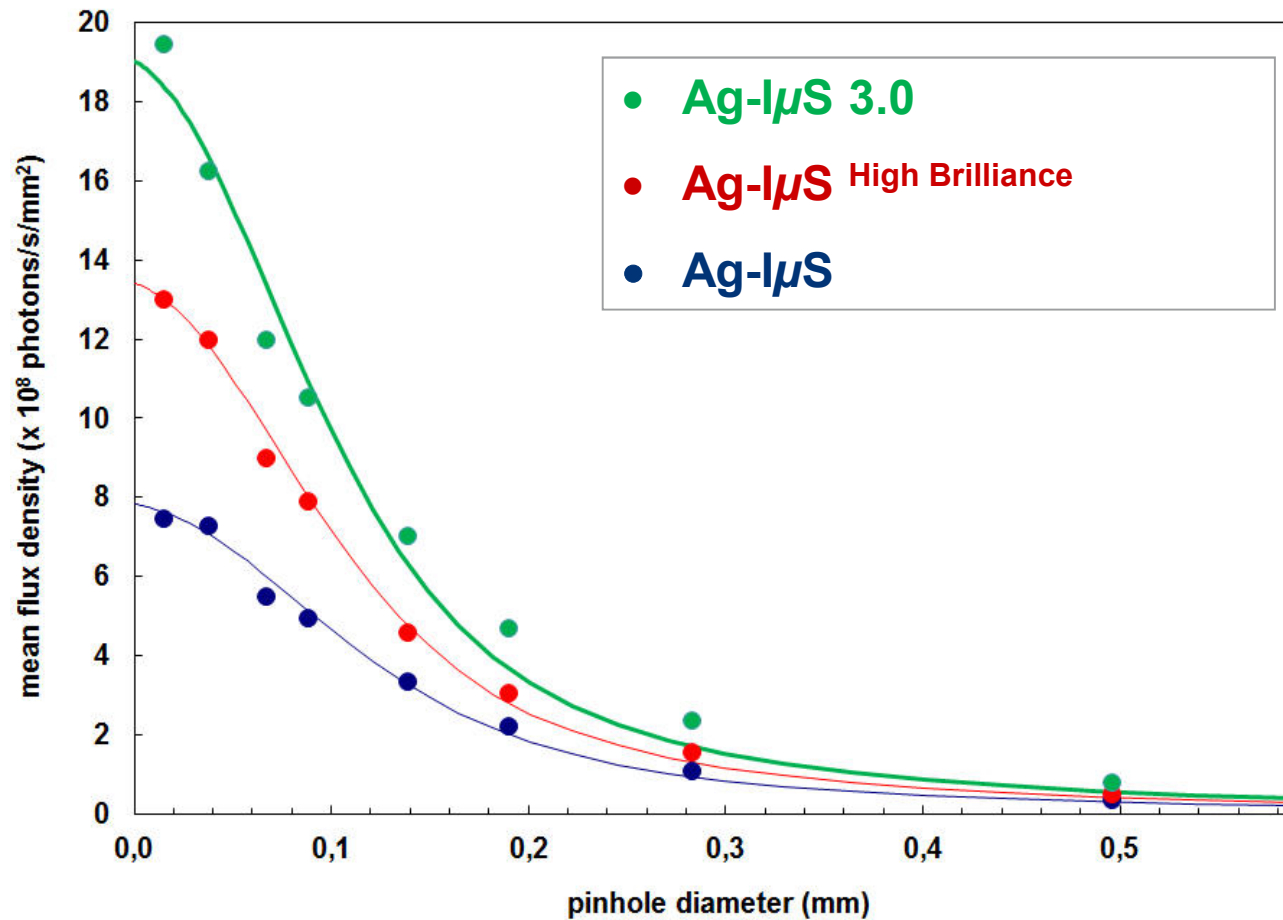


Mo-I $\mu$ S plus PHOTON100,  
resolution 0.64 Å,  $\pm 0.25$  e/Å<sup>3</sup>

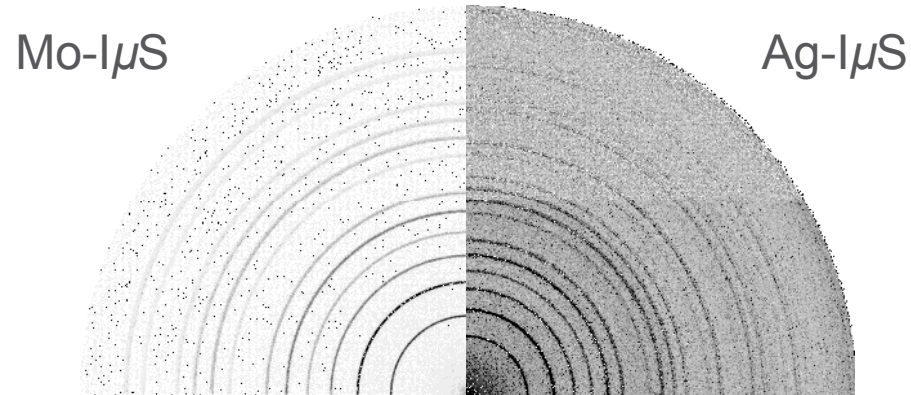


Mo-I $\mu$ S 3.0 plus PHOTON II,  
max. resolution < 0.56 Å,  $\pm 0.25$  e/Å<sup>3</sup>

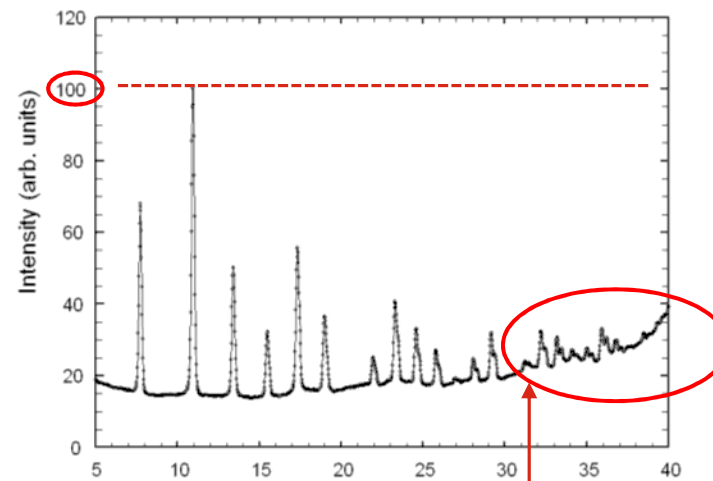
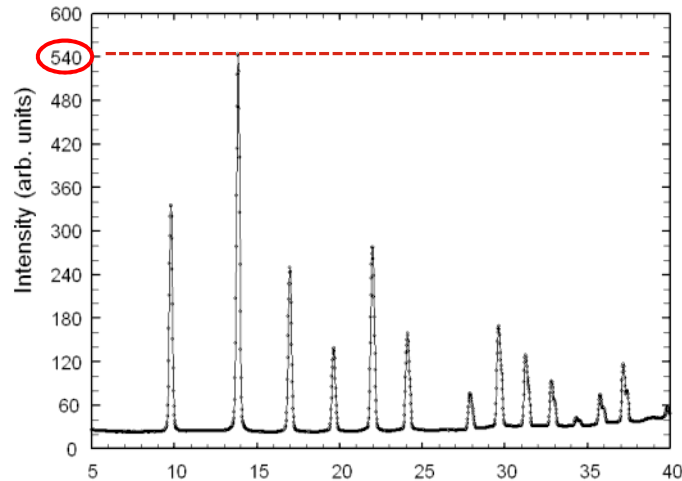
## Flux through pinholes w/ different diameter (calibrated PN diode)



# Which Wavelength to Use?



LaB<sub>6</sub> Sample in Capillary  
Exposure Time: 300 s  
Detector-Distance: 200 mm

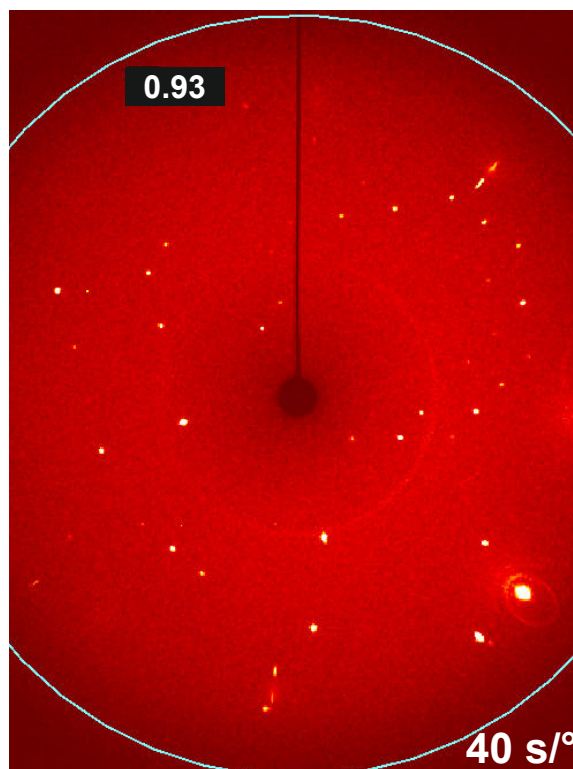


**Ag-K $\alpha$  for low absorbing materials:  
2x More Data, but Less Diffracted Intensity**

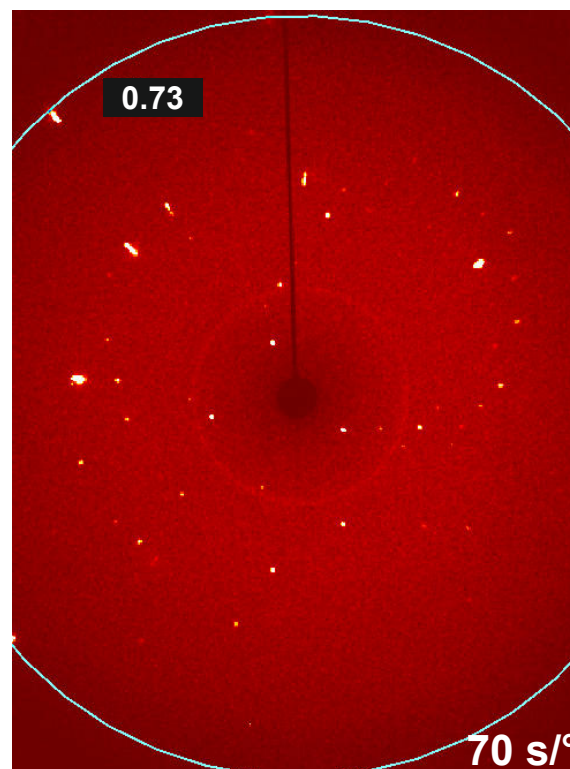
End of measurement range for Mo-K $\alpha$

## Purely Organic Small Molecule Compound in a DAC

Mo- $\mu$ S 3.0



Ag- $\mu$ S 3.0



Accessible Data

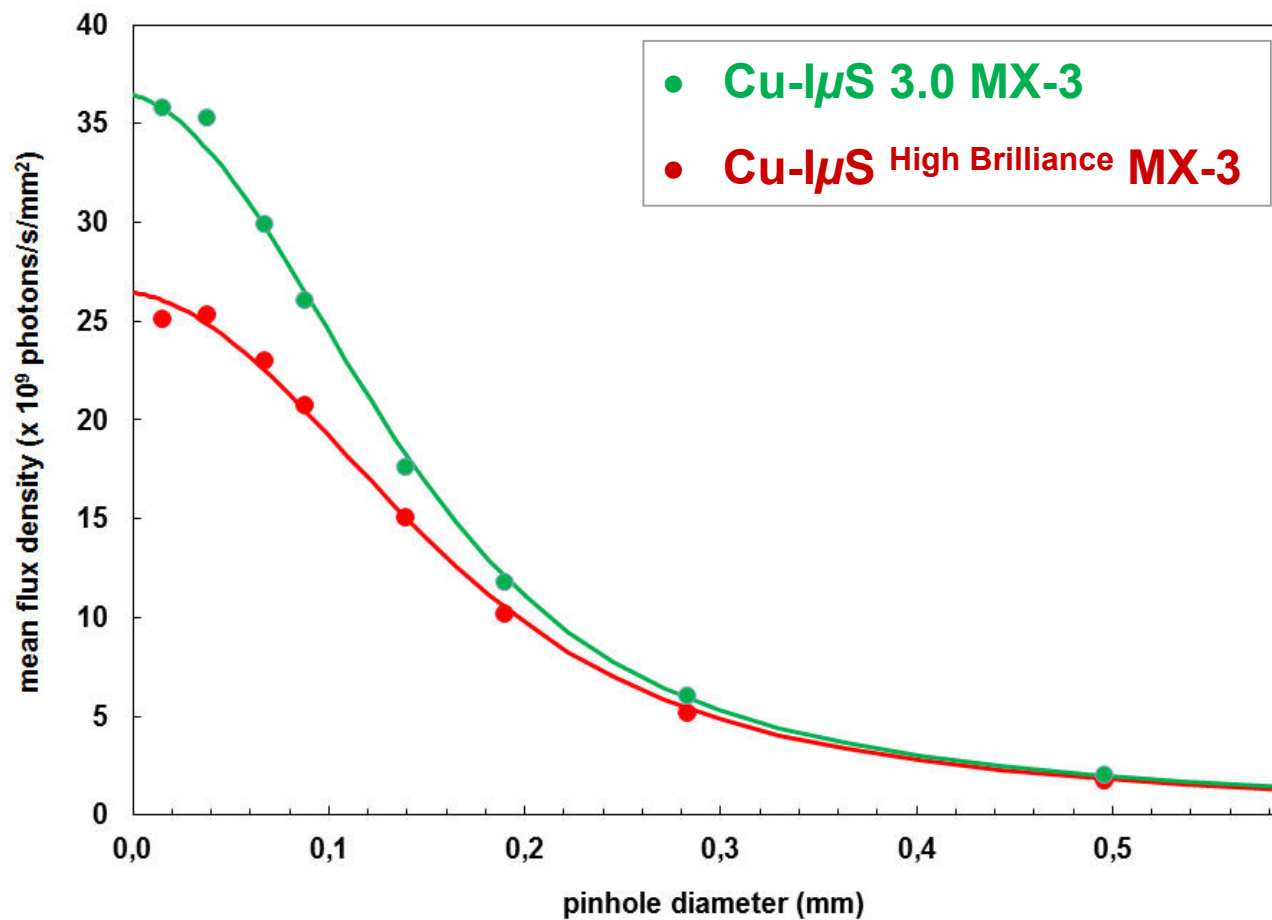
1

2

## Comparison of High-Pressure Data from a Purely Organic Compound

Source	Mo- $\mu$ S 3.0	Ag- $\mu$ S 3.0
Exposure time	40 s/°, <b>12 h</b>	70 s/°, <b>22 h</b>
Max. Access. Res.	0.65 Å	0.50 Å
Max. Res. [Å]	<b>0.65</b>	<b>0.58</b>
# Unique	<b>368 (47)</b>	<b>686 (174)</b>
Resolution [Å]	0.65 (0.75 – 0.65)	0.65 (0.75 – 0.65)
Completeness [%]	<b>21.9 (8.3)</b>	<b>32.8 (24.8)</b>
Multiplicity	3.8 (0.8)	5.4 (2.9)
$\langle I/\sigma \rangle$	<b>91.8 (16.8)</b>	<b>48.0 (8.2)</b>
$R1(\text{all}), wR2(\text{all})$ [%]	3.89, 11.77	4.05, 10.94
$d(\text{C-C})$ [Å]	<b>1.524(11)</b>	<b>1.516(6)</b>

## Flux through pinholes w/ different diameter (calibrated PN diode)

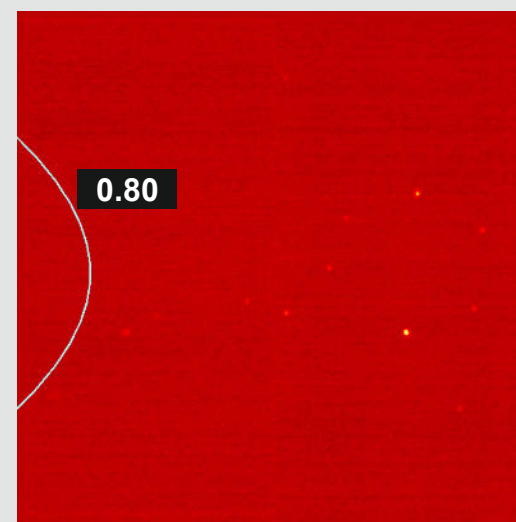
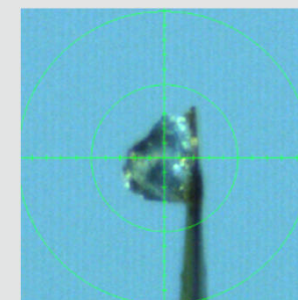


# Cu- $\mu$ S HB vs. Cu- $\mu$ S 3.0

## Real Life Example: Diphenyloxazolidin-2-one Derivate

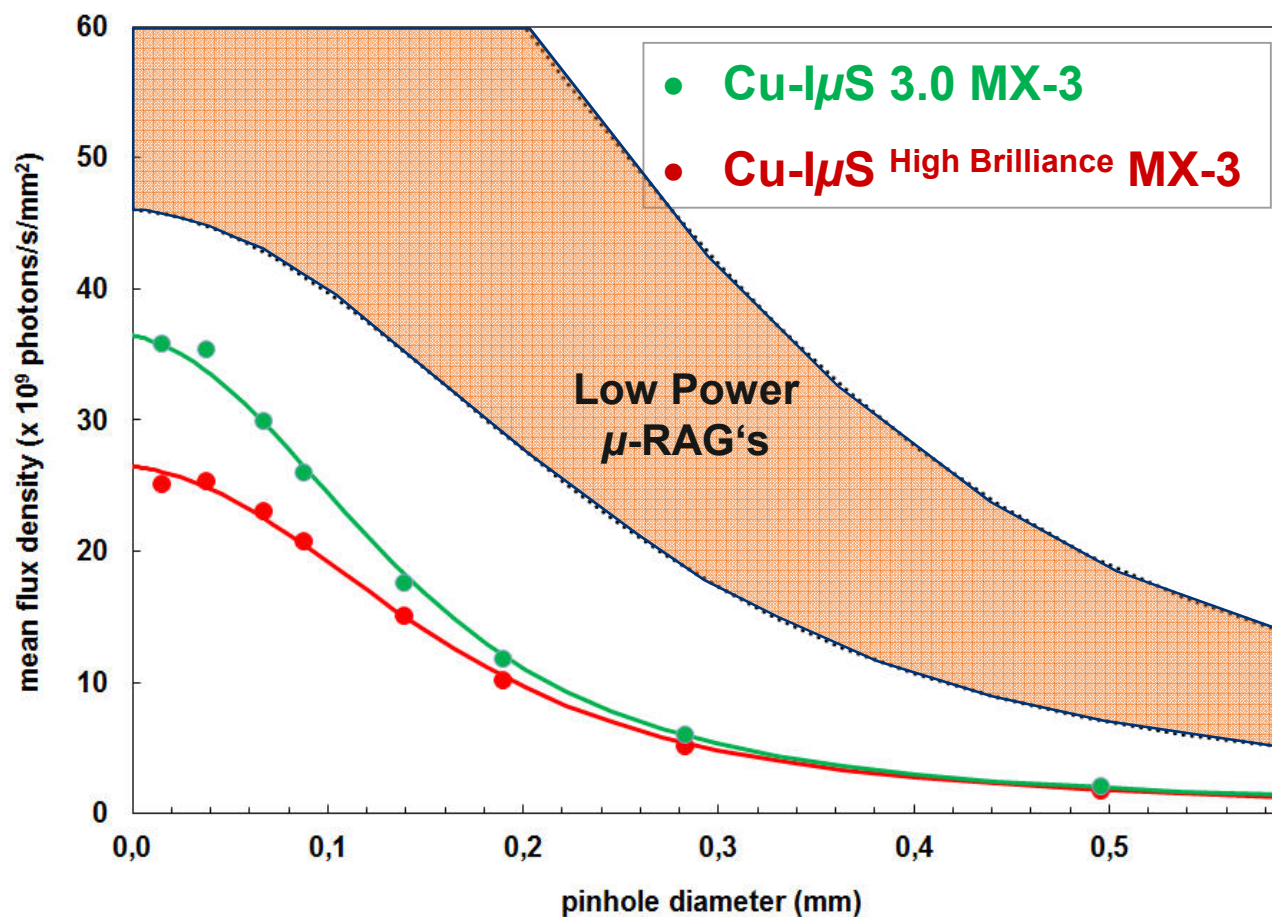
Source	Cu- $\mu$ S HB	Cu- $\mu$ S 3.0
Detector	PHOTON100	PHOTON100
Exposure time	4 – 12 s/°, <b>5 h</b>	4 – 12 s/°, <b>5 h</b>
Resolution [Å]	<b>0.78</b> (0.88 – 0.78)	<b>0.78</b> (0.88 – 0.78)
Multiplicity	<b>10.8 (7.5)</b>	<b>10.7 (7.5)</b>
$\langle I/\sigma \rangle$	<b>27.7 (11.7)</b>	<b>32.2 (14.8)</b>
R1, wR2 [%]	3.88; 9.88	<b>3.61; 9.20</b>
d(C-C) [Å]	1.386(4)	<b>1.389(3)</b>
Parsons z(v)	<b>0.07(9)</b>	<b>0.05(7)</b>

C<sub>25</sub>H<sub>31</sub>NO<sub>5</sub>, 0.12 x 0.10 x 0.09 mm<sup>3</sup>,  
comparable strategies

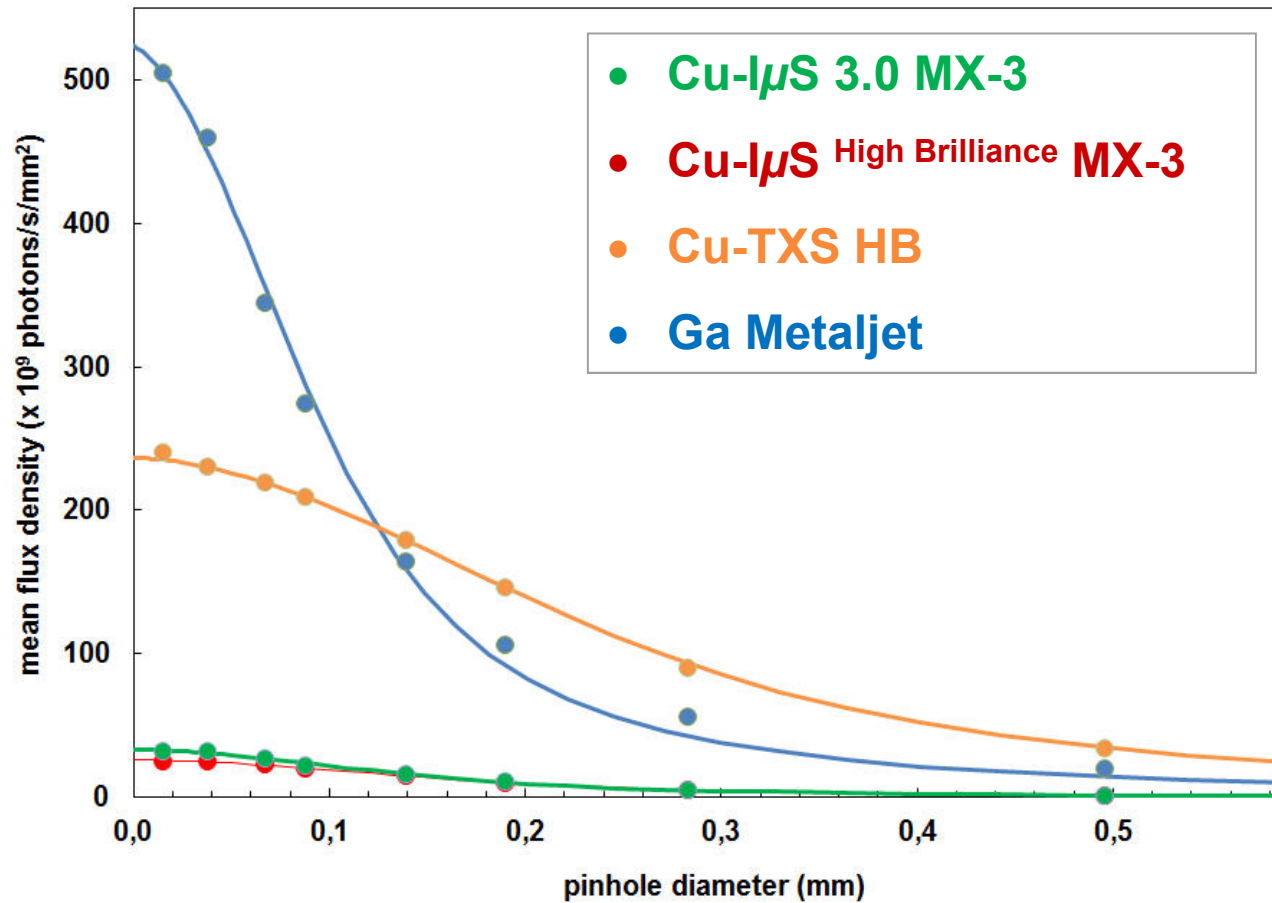


Typical diffraction pattern ( $P2_12_12_1$ ,  
 $a = 8.4167(17)$  Å,  $b = 13.761(3)$  Å,  
 $c = 19.304(4)$  Å,  $Z = 4$ )

## Flux through pinholes w/ different diameter (calibrated PN diode)

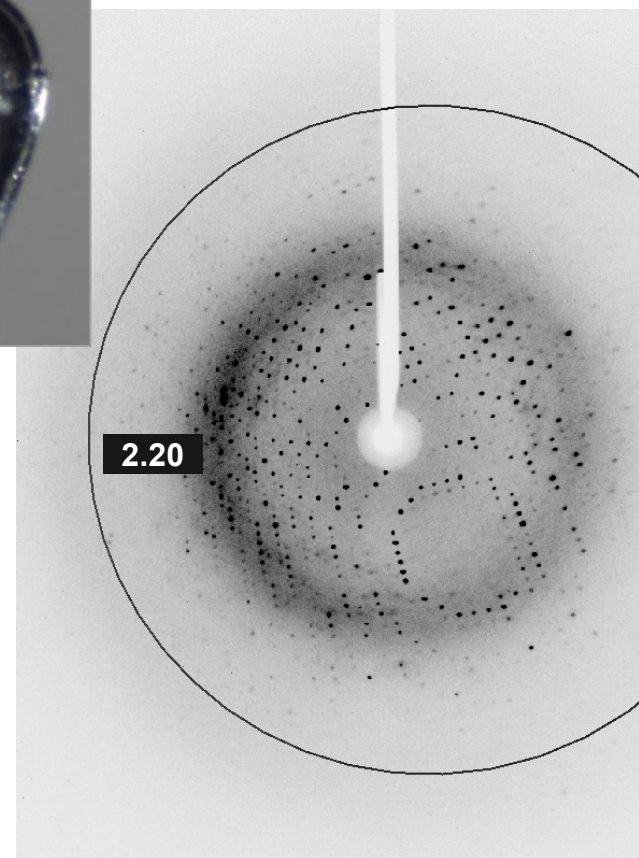


## Flux through pinholes w/ different diameter (calibrated PN diode)



## 215° Data Collection on Thin Crystal of Human NEIL1 (Endonuclease VIII-like protein)

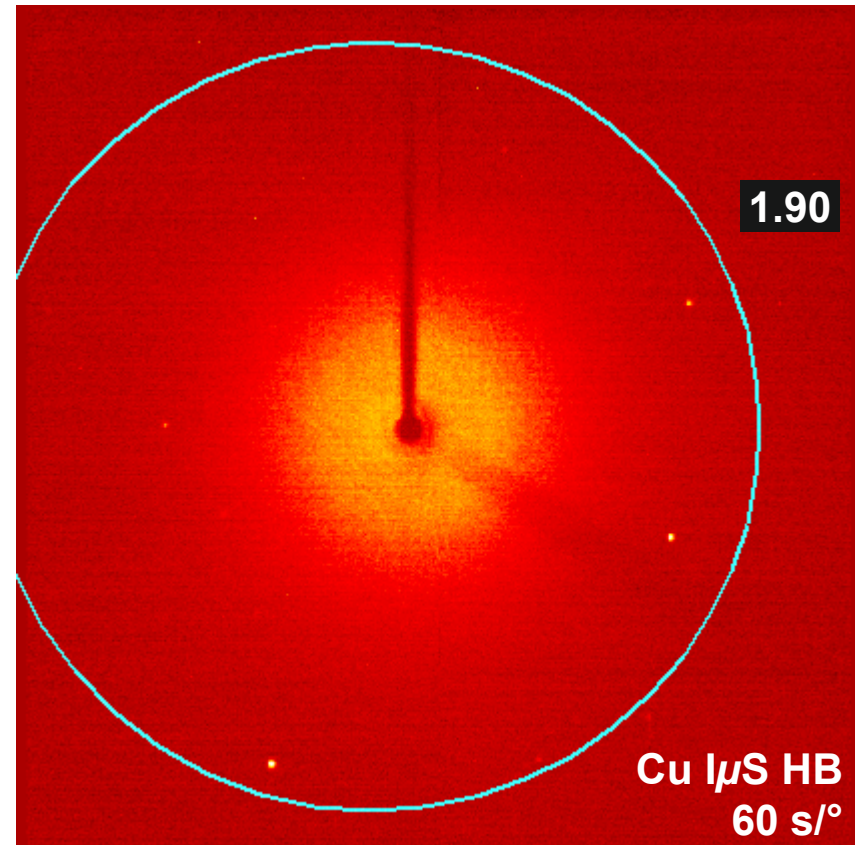
- Space group: *H3*
- Crystal size 0.15 x 0.12 x 0.02 mm<sup>3</sup>
- Resolution on  $\mu$ -RAG ~ 2.6 Å



Source	Cu- $\mu$ S 3.0
Exposure time	100 s/0.5°
Total time [h]	12
Resolution [Å]	2.25 (2.32 – 2.25)
Completeness [%]	99.6 (99.7)
Multiplicity	5.1 (3.5)
$\langle I/\sigma(I) \rangle$	13.2 (2.6)
$R_{\text{merge}}$	7.07 (32.34)
CC <sub>1/2</sub> at High res	89%

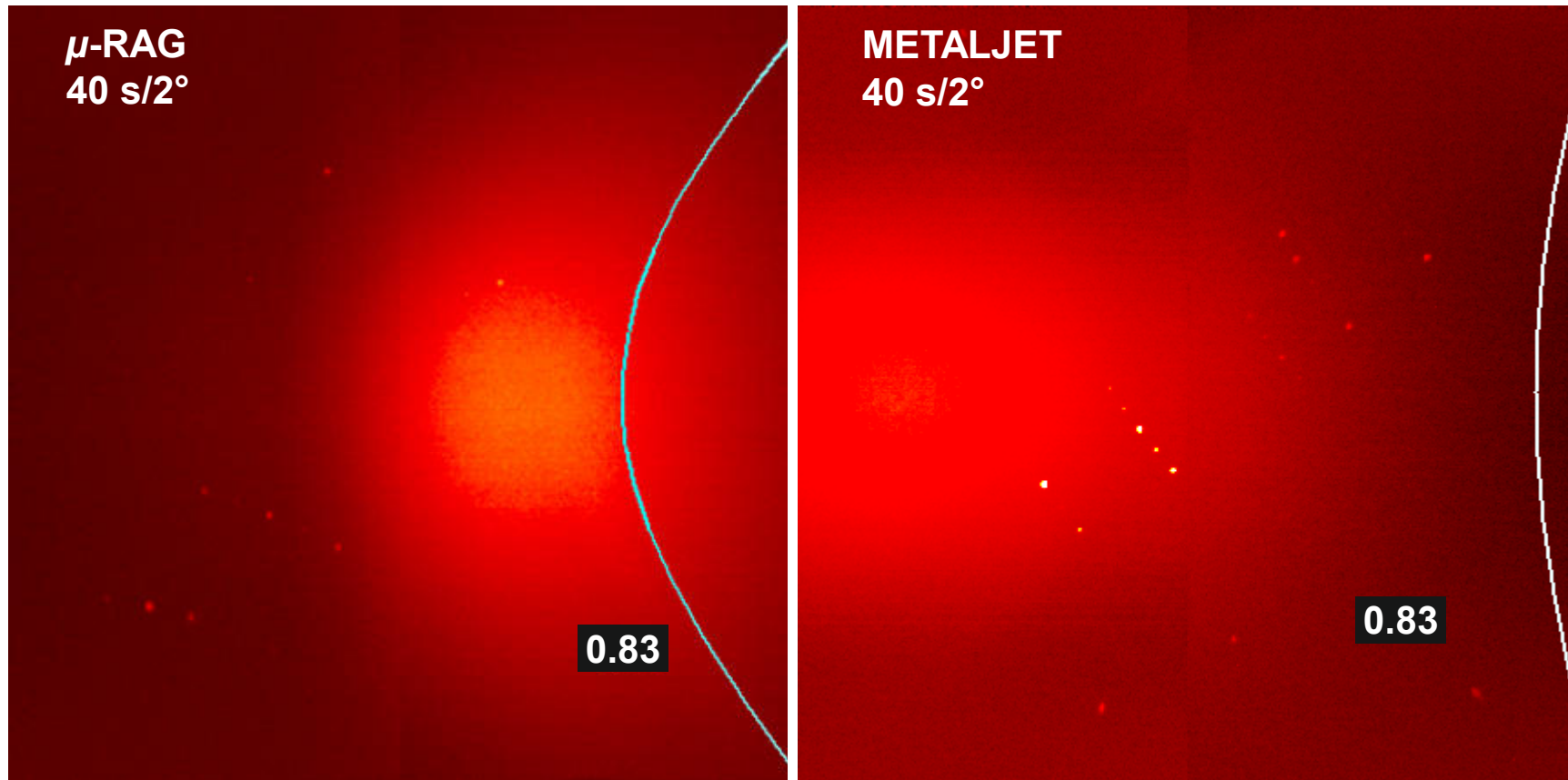
# How Small? – Testing the Limits

## Typical Diffraction Patterns from a 0.03 x 0.02 x 0.01 mm<sup>3</sup> Crystal (Purely Organic)



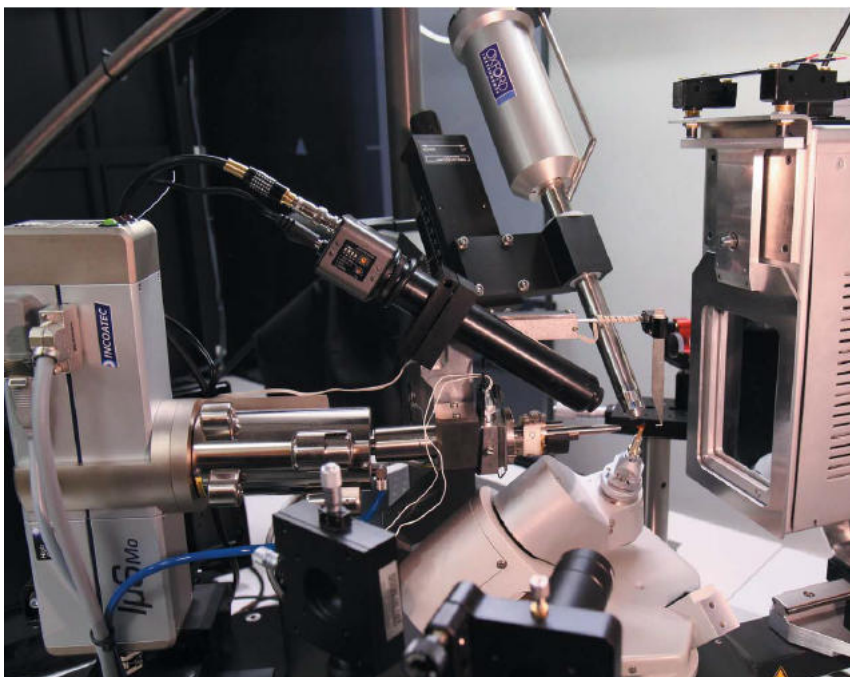
# How Small? – Testing the Limits

## Perfect Sample for Diffraction on High-Brightness X-ray Source

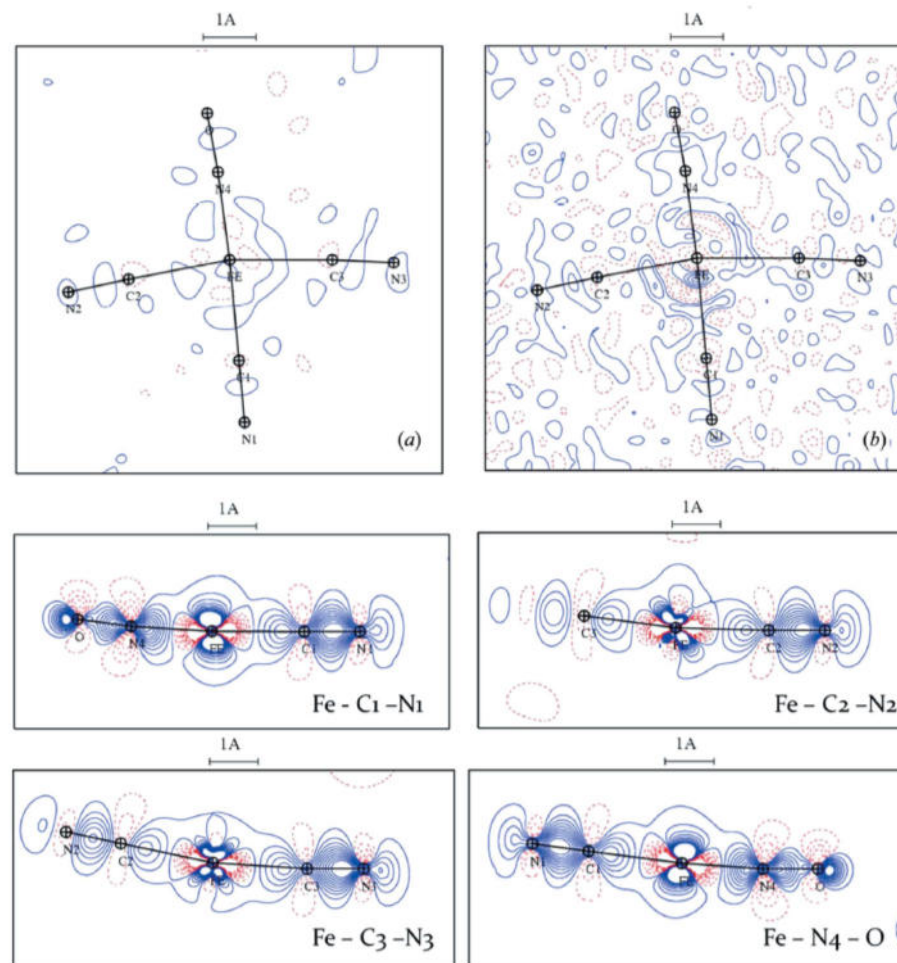


# Many More Applications: Charge Density

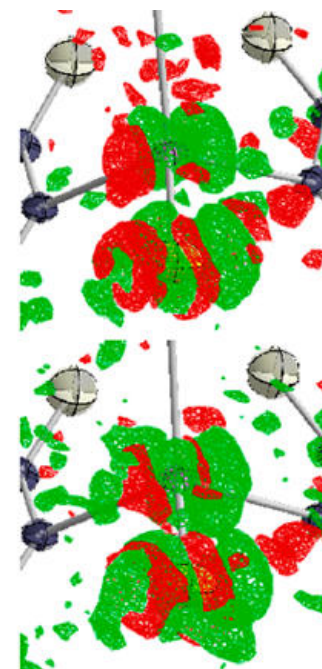
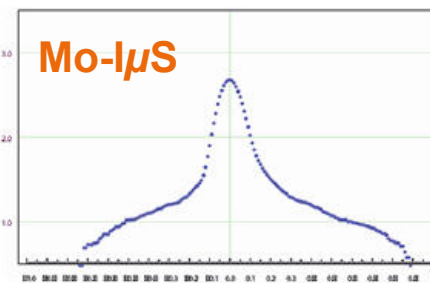
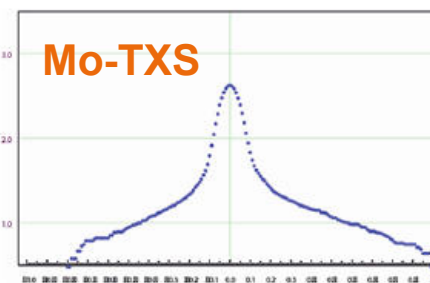
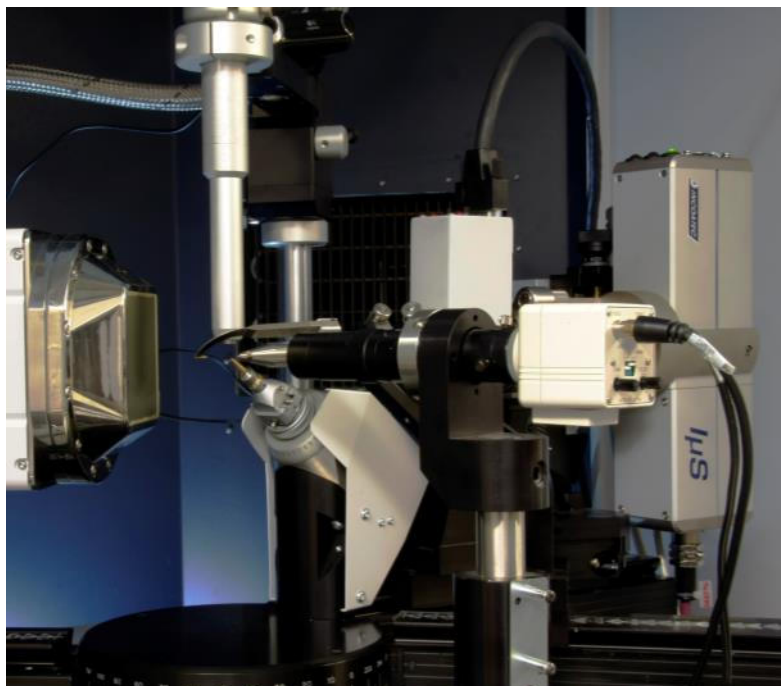
## Charge density study on a sodium nitroprusside crystal



Dr. E. Wenger, Prof. D. Schaniel,  
Prof. C. Lecomte,  
Université de Lorraine, Nancy



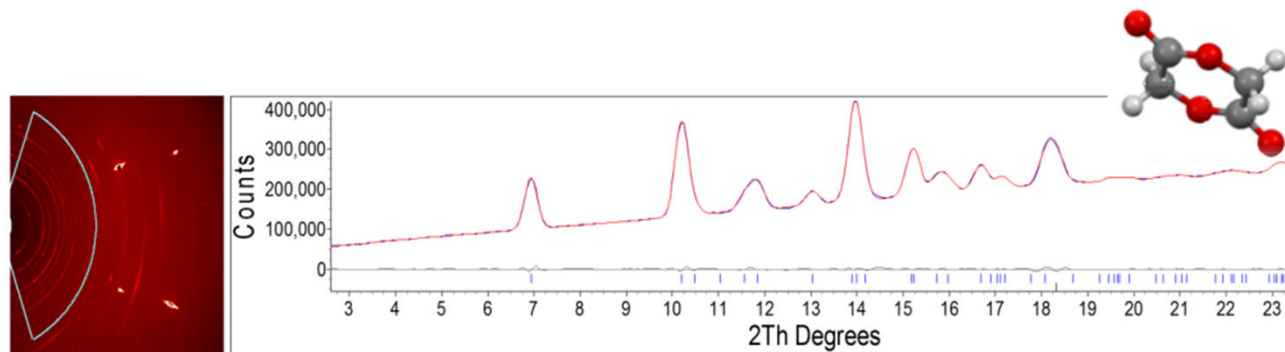
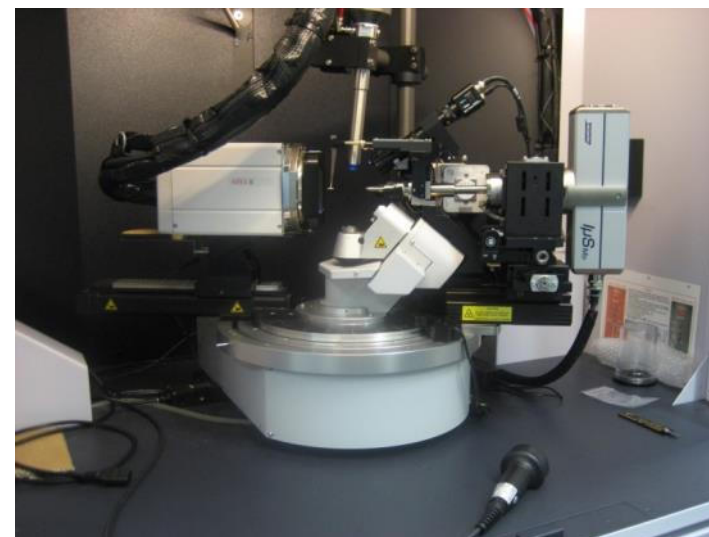
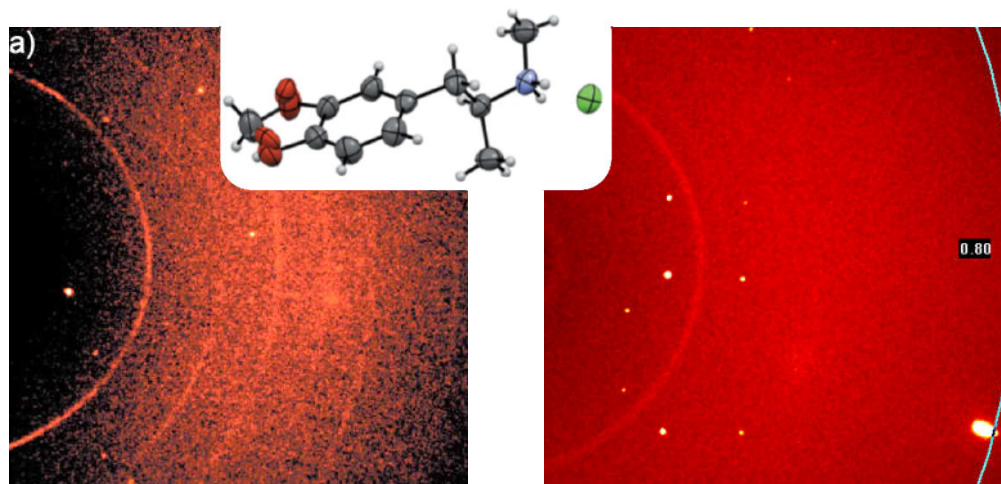
## Charge density study on a 9-diphenyl-thiophosphinoyl-anthracene crystal: Comparison Mo- $\mu$ S vs. Mo-TXS data



Dr. R. Herbst-Irmer, Prof. D. Stalke,  
Georg-August-Universität Göttingen

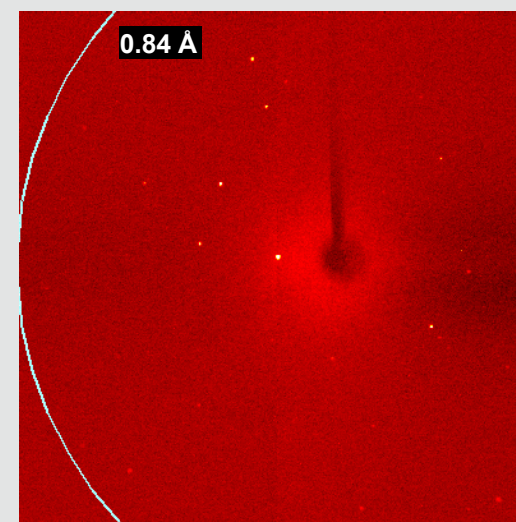
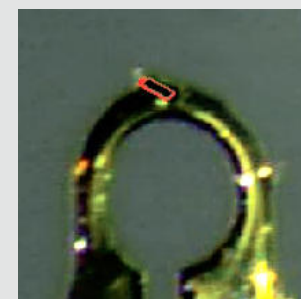
# Many More Applications: High-Pressure XRD

## Single Crystal and Powder Diffraction Studies of Pharmaceutical Compounds under High Pressure



## Tiny Crystal of MOF Compound

Size [mm <sup>3</sup> ]	0.018 x 0.010 x 0.002
Source	Mo-I $\mu$ S HB
Power [W]	50
Exposure time	240 s/ $^{\circ}$ , 22 h
Resolution [Å]	0.83 (0.93 – 0.83)
Multiplicity	3.9 (2.2)
$\langle I/\sigma \rangle$	15.1 (4.2)
R1, wR2 [%]	4.27; 8.83



Typical diffraction pattern ( $P2_1/m$ ,  
 $a = 8.9215(10)$  Å,  $b = 21.209(2)$  Å,  
 $c = 9.1052(10)$  Å,  $\beta = 107.923(3)^\circ$ ,  $Z = 2$ )



## Application Note SC-XRD 502

### Structural Determination of a Two Micron-sized MOF Crystal

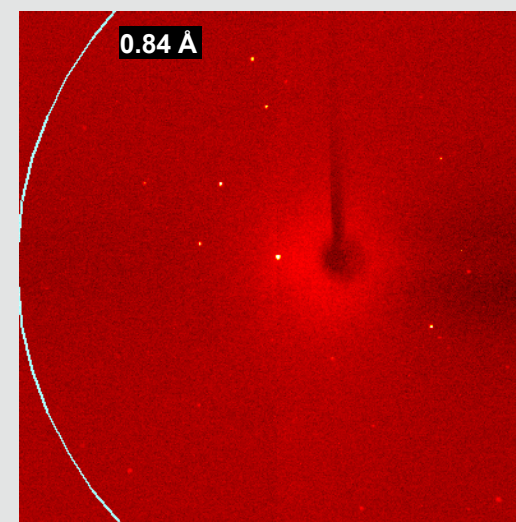
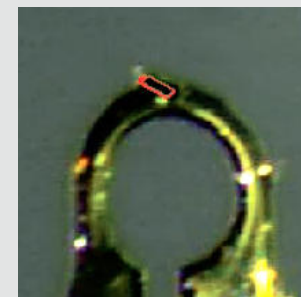
Metal-Organic Frameworks (MOFs) are structures of great industrial and academic interest as they can be at the genesis of a series of new materials with highly attractive properties. Nowadays MOFs can be prepared very fast, under mild conditions in high yields while still combining several functions, taking advantage of the metallic centers, the organic ligands and the framework itself. Some MOFs can even outperform known materials in common industrial applications.

[La(H<sub>2</sub>bmt)(H<sub>3</sub>bmt)(H<sub>2</sub>O)<sub>2</sub>·3H<sub>2</sub>O (**1**)] has outstanding catalytic activity for the methanolysis of styrene oxide in comparison to that of related MOF-type heterogeneous catalysts. In addition, the inclusion of small amounts of other lanthanides can produce highly photoluminescent materials.<sup>11</sup> **1** can be quickly prepared in 5 minutes at 330 K using microwave-assisted synthesis from the tridentate (benzene-1,3,5-triyltris(methylene)triphosphonic acid (H<sub>3</sub>bmt) and LaCl<sub>3</sub>·7H<sub>2</sub>O. Nevertheless, to fully understand

microscope. The D8 VENTURE consists of a KAPPA goniometer and PHOTON 100 CMOS APS detector, equipped with a 1μS microfocus X-ray source providing Mo-Kα radiation (λ = 0.71073 Å). During the entire experiment the sample was kept at 100 K using a KRYOFLEX II low temperature device, controlled with the APEX2 software package.

#### The experiment

Based on a number of initial scans the unit cell determination routine of the software suite indicated a monoclinic unit cell. From the same scans 0.5 degree frames were suggested by the data collection strategy optimizer and the refined data collection strategy consisted of only three scans. Due to the weak diffraction of this very tiny crystal, an appropriate frame exposure time of 120 s was selected. A total of 645 frames were collected within just 21.5 hours.



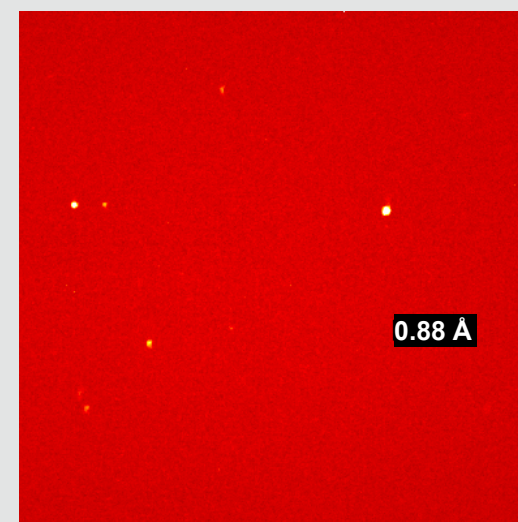
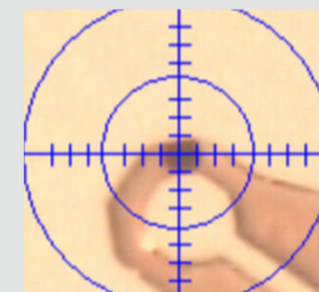
Typical diffraction pattern ( $P2_1/m$ ,  
 $a = 8.9215(10)$  Å,  $b = 21.209(2)$  Å,  
 $c = 9.1052(10)$  Å,  $\beta = 107.923(3)^\circ$ ,  $Z = 2$ )

# How Small? – If You Don't Get Data w/ Mo-I $\mu$ S...

Tiny Crystal of a MOF Compound:

No Diffraction w/ Mo-I $\mu$ S, but w/ **Cu-I $\mu$ S MX**

Size [mm <sup>3</sup> ]	0.03 x 0.02 x 0.01
Source	Cu-I $\mu$ S MX
Power [W]	30
Exposure time	60 – 120 s/0.5°
Resolution [Å]	<b>0.88</b> (0.98 – 0.88)
$\langle I/\sigma \rangle$	<b>16.2</b> (3.4)
R1, wR2 [%]	5.3, 13.6



Typical diffraction pattern with Cu-I $\mu$ S MX  
(P4<sub>2</sub>/n, 120 s/0.5°, APEX II DUO)

# Many More Applications: High-Throughput Fragment Screening

## How much data is needed for finding the ligand?

Influence of completeness on the quality of the electron density map around the small molecule fragment ( $C_8H_9N_2SCl$ )



1 h Data set

60% completeness,  
Multiplicity 0.9,  $\langle I/\sigma \rangle$  10.1



1.3 h Data set

80% completeness,  
Multiplicity 1.4,  $\langle I/\sigma \rangle$  13.0



3.5 h Data set

96% completeness,  
Multiplicity 1.8,  $\langle I/\sigma \rangle$  18.0

**Electron density maps of high quality within a short period of time**

# Many More Applications: High-Throughput Fragment Screening

## How much data is needed for finding the ligand?

Influence of completeness  
small molecule fragment



1 h Data set

60% completeness,  
Multiplicity 0.9,  $\langle I/\sigma \rangle 10.1$

### Application Note 6

#### Fragment Screening Using a Twinned Protein Crystal

##### Introduction

Fragment-based screening using X-ray crystallography has become one of the major techniques in contemporary drug design. The aim of fragment screening is to run a rapid data collection of a protein crystal in complex with a small fragment molecule, in order to find out whether the fragment has bound to an active site of the protein or not. The increasing popularity benefits from recent developments of highly brilliant X-ray sources as well as fast and sensitive area detectors. This allows high quality data to be collected within a reasonable period of time using a large number of different fragment chemotypes. This is especially beneficial if one wants to screen a fragment library.

Here, we present results that were obtained by collecting data from a twinned endosthepsin crystal in complex with a small fragment molecule. The influence of the data completeness on the quality of the obtained electron density maps was analyzed, in order to find the minimum data collection time that is needed to detect the inhibitor in the active site.

resolution of 2.6 Å. The data was processed to 60%, 80% and 96% completeness, resulting in data sets with total collection times of 1 h, 1 h 20 min and 3 h 30 min. The electron density map around the active site was inspected to see whether the fragment was bound. The data collection was performed using a Bruker AXS X8 PROSPECTOR equipped with an Incoatec Microfocus Source  $\mu\text{S}$  with QUAZAR MX optics and an APEX II detector (Fig. 1). Data collection and processing were performed with the PROTEUM2 suite [1].

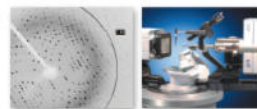


Figure 1. Diffraction pattern of the endosthepsin crystal (left; 15  $\times$  10  $\mu\text{m}^2$ ), X8 PROSPECTOR with a Cu- $\mu\text{S}$  microfocus X-ray source equipped with a QUAZAR MX optics and APEX II detector (right).

density map around the



3.5 h Data set

96% completeness,  
Multiplicity 1.8,  $\langle I/\sigma \rangle 18.0$

Electron density maps of high quality within a short period of time

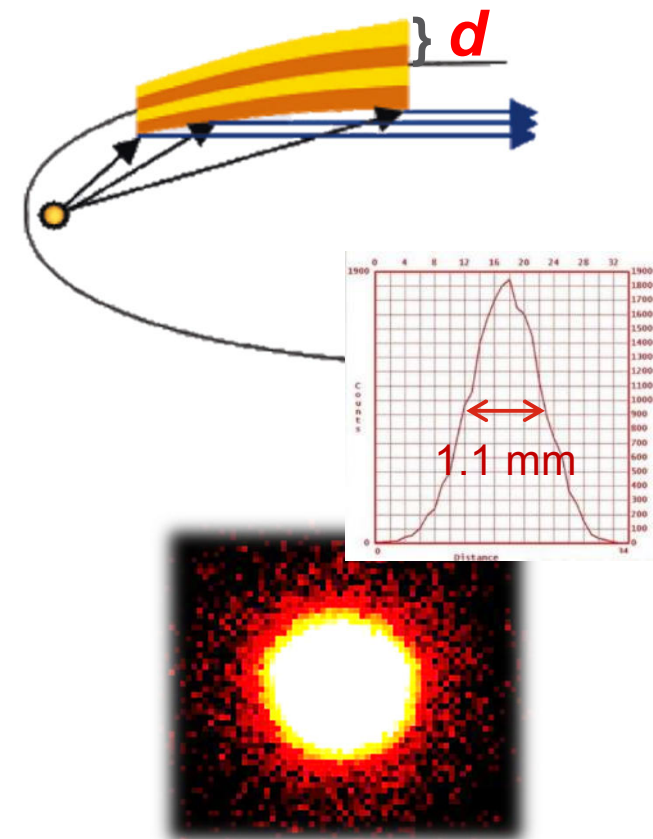
## Characteristics of the $\mu$ S for XRD and SAXS

### ■ Parallel Beam Multilayer Optics

- High-resolution XRD and SAXS
- Typical energies: Cu, Co, Mo, Ag
- Typical FWHM at the sample  $\sim 1 - 2$  mm
- Typical divergence:  $\leq 1$  mrad

### ■ Focusing Multilayer Optics

- Spatially resolved XRD
- Typical energies: Cu, Cr, Mo, Ag



## Raw Flux Comparison on a Bruker NANOSTAR

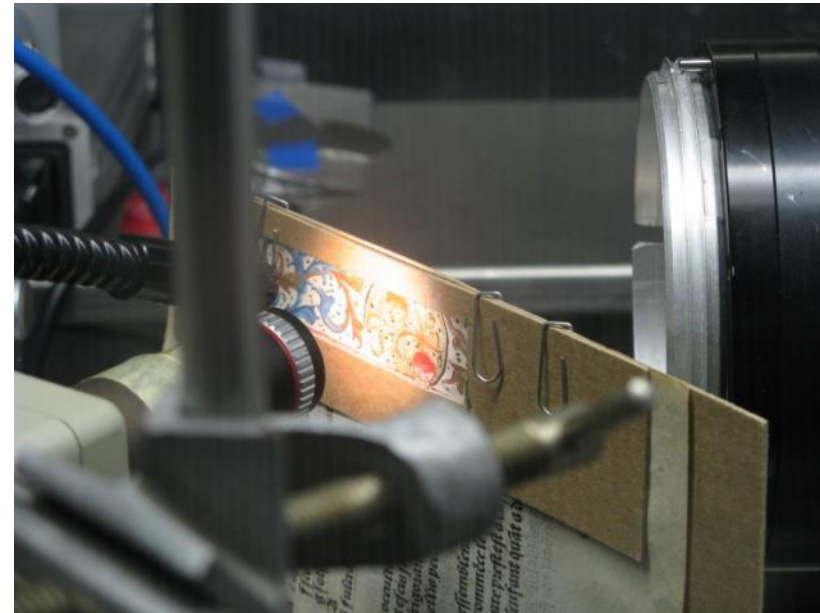
- $1\mu\text{S}$  (30 W, Standard Set-up):  $1.5 \times 10^7$  cps

## Relative Intensities (Sources w/ ML Mirrors)

- ST + cc-Göbel mirrors (1.4 kW, FF): 1
- $1\mu\text{S}$  (30 W,  $0.04 \times 0.20 \text{ mm}^2$ ): 7
- $1\mu\text{S}$  HB (50 W,  $0.04 \times 0.40 \text{ mm}^2$ ): 8
- RAG (4.0 kW,  $0.3 \times 3 \text{ mm}^2$ ): 8
- $\mu$ -RAG (1.2 kW,  $0.1 \times 1 \text{ mm}^2$ ): 15
- METALJET (200 W,  $0.02 \times 0.08 \text{ mm}^2$ ): > 100
- METALJET with scatter-free pin-holes: > 250

Note that same parallel beam mirror type and resolution settings were used for all data from microfocus X-ray sources.





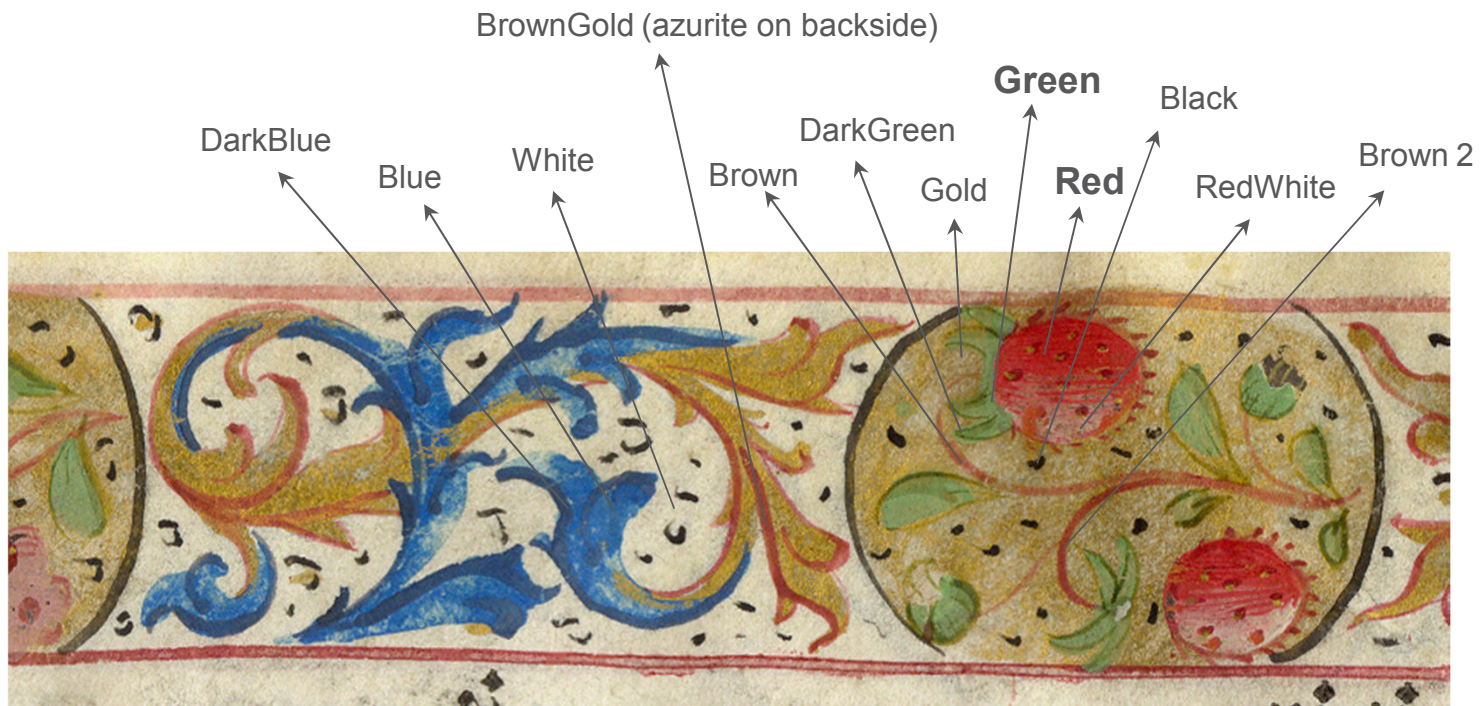
**Simultaneous XRD and XRF measurements**

**Position sensitive measurements using focusing Mo- $\mu$ S**

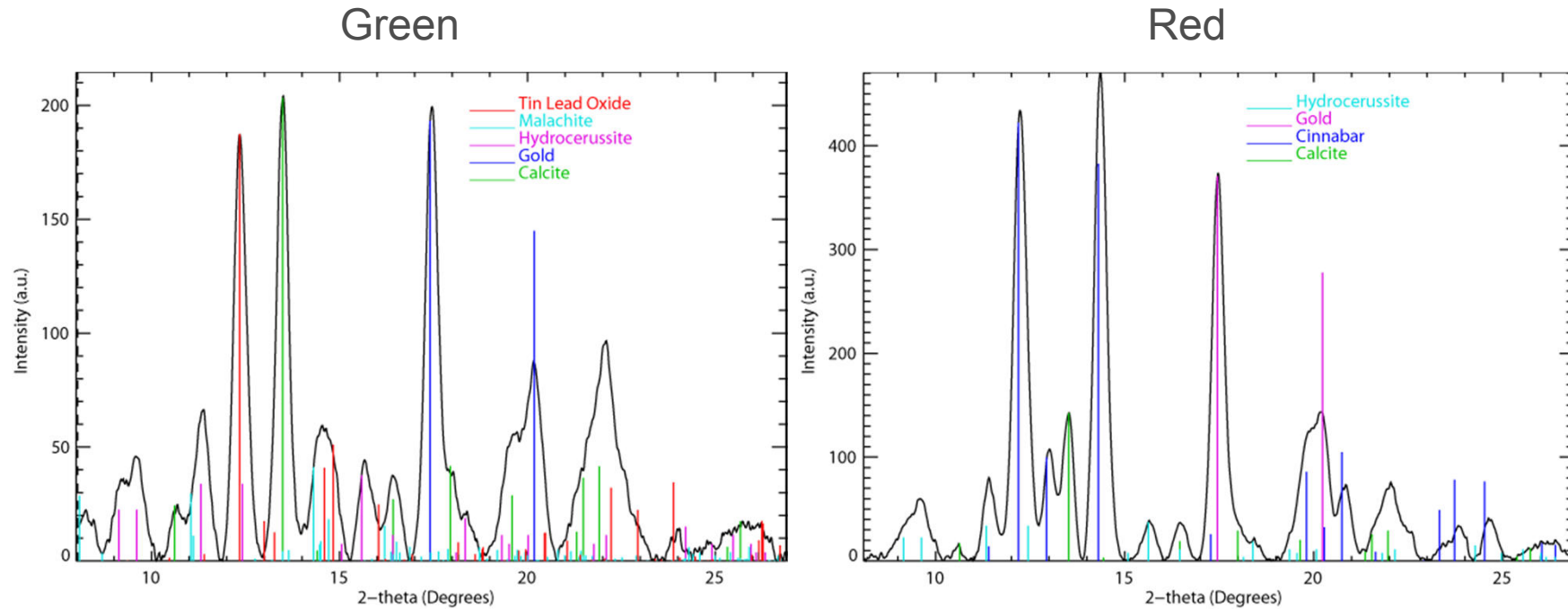
- Resolution 150  $\mu$ m

K. Janssens, F. Vanmeert, Antwerpen

# Illuminated Manuscript Point Measurements

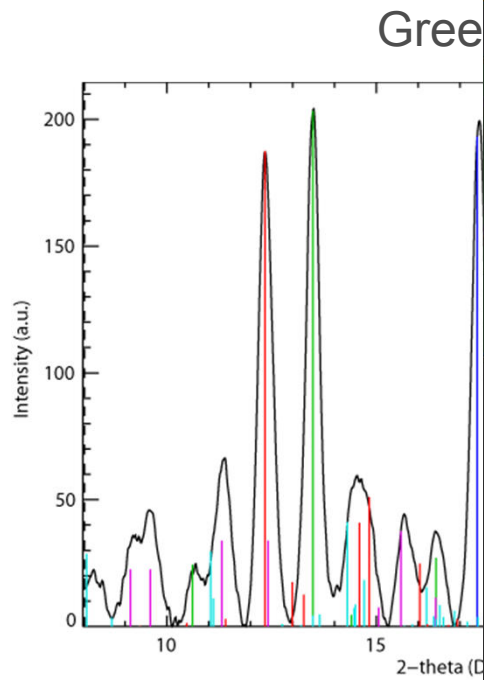


K. Janssens, F. Vanmeert, Antwerpen



- Mo-I $\mu$ S: 50 kV, 600  $\mu$ A, 30 sec exposure time
- Scanning Micro diffraction (combined with XRF):
  - 4 x 4.5 mm<sup>2</sup>, resolution 150  $\mu$ m, Total measurement time: 18 h
- Measurements and data evaluation by Frederick Vanmeert

K. Janssens, F. Vanmeert, Antwerpen



- Mo- $\mu$ S: 50 kV, 600
- Scanning Micro diffractometer
- Measurements and analysis on a  $4 \times 4.5 \text{ mm}^2$  area

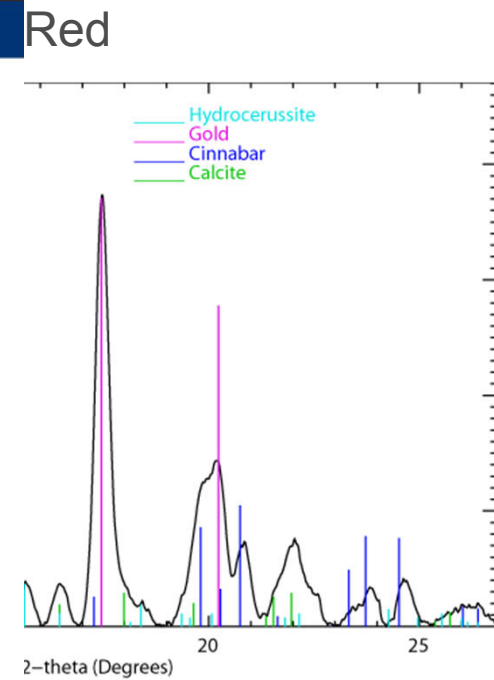
K. Janssens, F. Vanmeert

## The Incoatec Microfocus Source $\mu$ S for XRD-Applications

### Microdiffraction using an $\mu$ S

Frederik Vanmeert, University of Antwerp has examined De Heem's painting 'Flowers and Insects', Royal Museum of Fine Arts Antwerp with the Incoatec Microfocus Source  $\mu$ S for XRD-Applications.

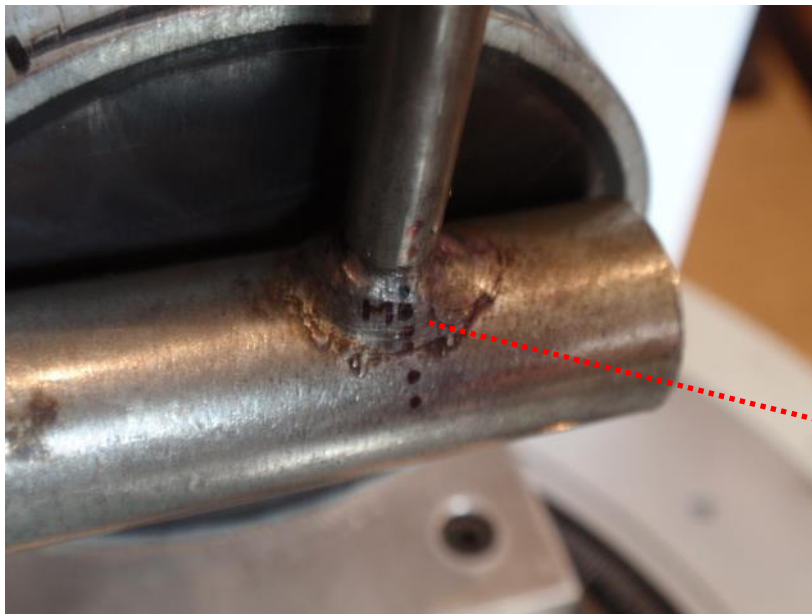
In recent years the interest in the non-destructive investigation of cultural heritage objects has risen strongly. Besides infrared and optical imaging and spectroscopic methods, X-ray methods like X-ray fluorescence, X-ray diffraction, X-ray radiography and X-ray imaging methods (e. g. tomography) are often used for the analysis of these artifacts [1]. Using for example X-ray fluorescence (XRF) the scrolls of Qumran were investigated [2], fragments could be identified as belonging together or not [3]. Using XRF analysis of paintings generally provides information about the possible presence of elements on the surface of art-objects due to pollution (e.g. sulphur or chlorine), about the elements and pigments used by the artist, about previous restored areas detected by the presence of "modern" elements like titanium or zinc, and identification of fraudulent submission. In combination with X-ray diffraction (XRD) also the crystallographic composition of the used pigments could be characterised. A study about the alteration involved the oxidation of cadmium yellow ( $\text{CdS}$ ) to  $\text{CdSO}_4 \cdot 2\text{H}_2\text{O}$  under the influence of light, oxygen and moisture is an example of the use of this technique in the investigation of paintings [1]. Other X-ray methods are used as well. A painting by Rembrandt van Rijn was analysed using an X-ray absorption imaging technique at ESRF and with XRF revealing an overpainting [4].



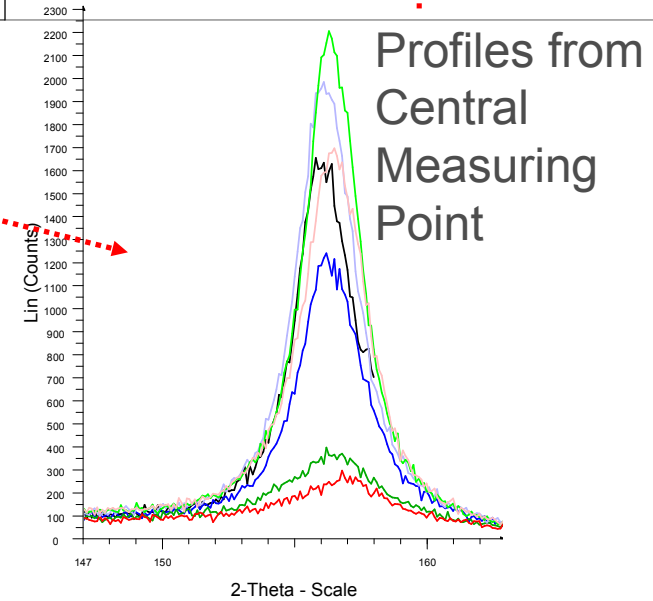
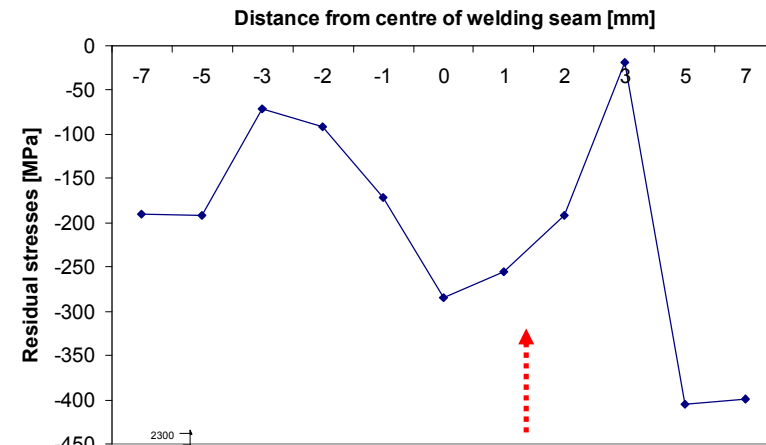
ne: 18 h

# $I\mu S$ (Cr-K $\alpha$ ) with focusing optics for Residual Stress measurements

Profile across a 6 mm weld seam



Measuring Steps 1mm

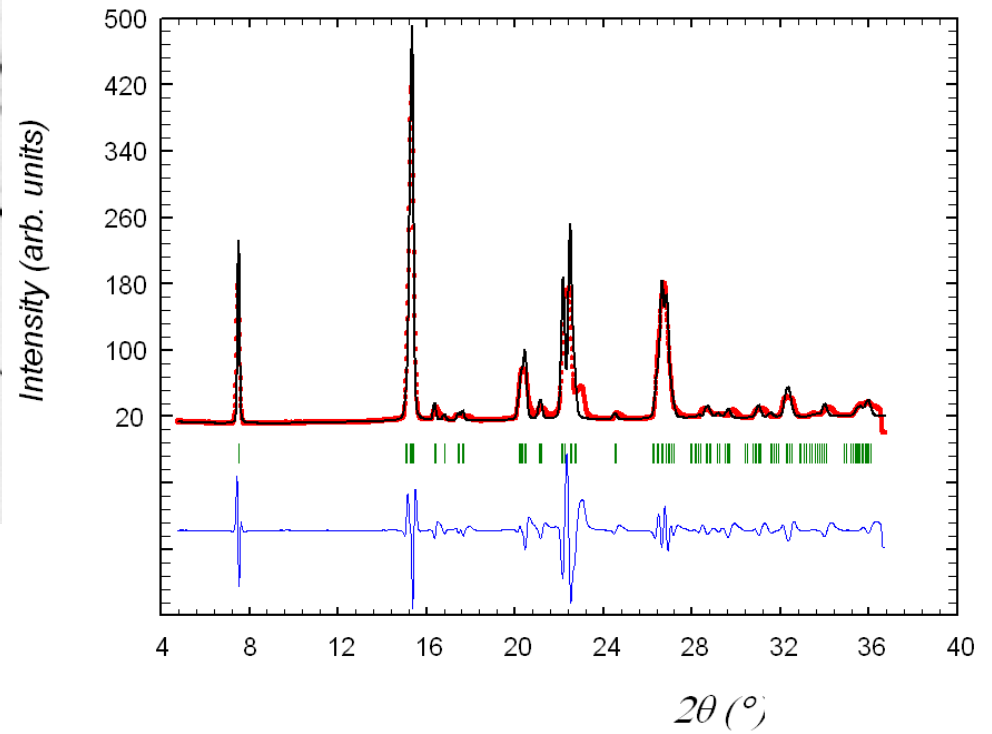


H. and U. Göbel, LabXA and M. Schuster, Siemens, Munich

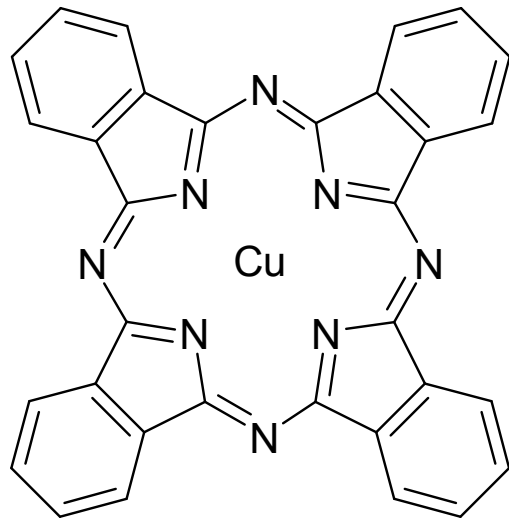
# ASS with Cu-K $\alpha$



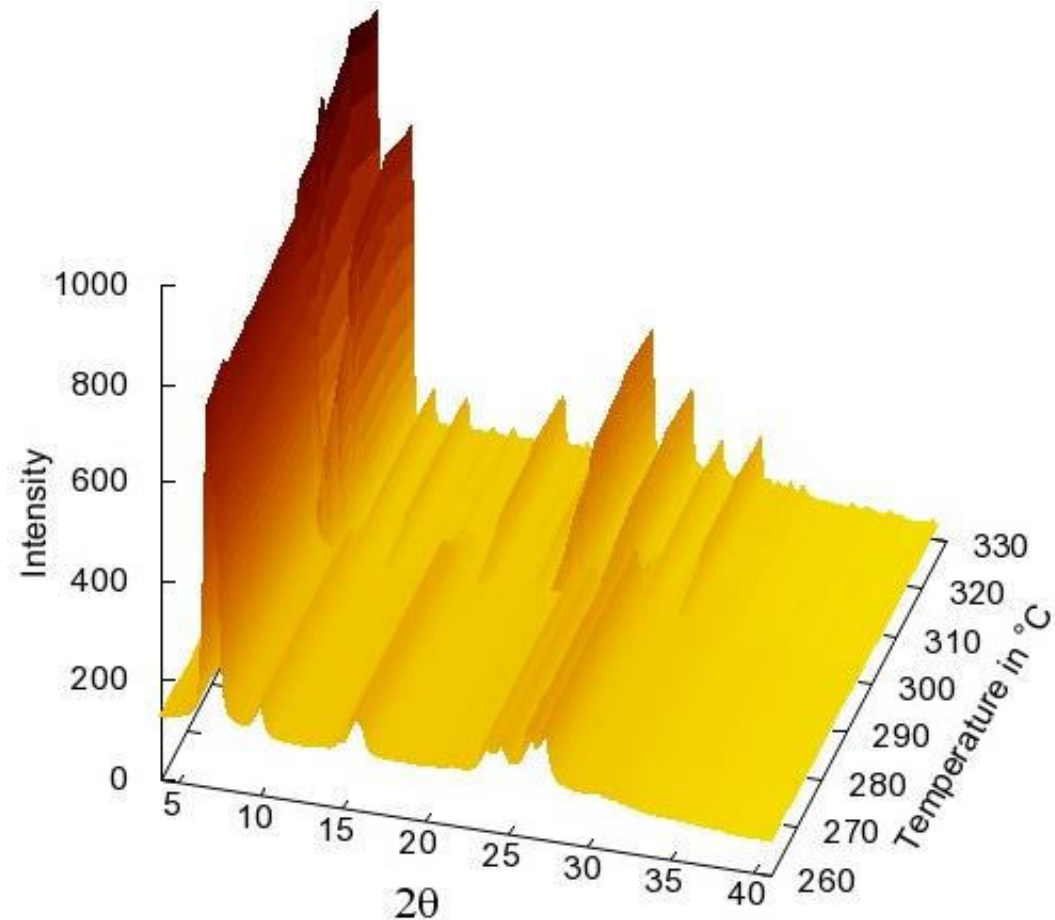
Whole tablet  
Exposure time: 300 s  
Focusing onto the detector



# Temperature-dependent Phase Transition in Copper Phthalocyanine



- Heating from 30 °C to 350 °C with a rate of 0.75 K/min
- Exposure time per frame: 240 s
- Operation mode of mar345: 100 μm x 100 μm @ 240 mm



R.E. Dinnebier, M. Müller, MPI for Solid State Research, Stuttgart

## ■ **$I\mu S$**

- Air-cooled low-power high-brightness microfocus X-ray source
- Intensity higher than conventional RAG, comparable to low-power  $\mu$ -RAG
- Different mirror designs allow for a wide range of applications
- Available for Cu-K $\alpha$ , Mo-K $\alpha$ , Ag-K $\alpha$  and also for Cr-K $\alpha$ , Co-K $\alpha$ , ...
- Upgrade for existing diffractometers, optional with its own enclosure IXE
- > 700 installations world wide

## ■ **NEW $I\mu S$ 3.0**

- First and only microfocus X-ray sealed tube optimized for X-ray diffraction
- New tube, new beampath concept, new optics
- 30 - 40% more intensity compared to the  $I\mu S$  HB
- No compromises on life-time and ease-of-use
- Available for Cu-K $\alpha$ , Mo-K $\alpha$  and Ag-K $\alpha$
- Available as upgrade of existing equipment
- Replacement for low power  $\mu$ -RAG's

# Acknowledgement



**I. Dix, T. Wagner, Novartis AG**

**B. Dittrich, Heinrich-Heine-Universität Düsseldorf**

**F. P. A. Fabbiani, Georg-August-Universität Göttingen**

**A. Heine, Philipps-Universität Marburg**

**C. W. Lehmann, MPI Mülheim**

**D. Stalke, G. Sheldrick, Georg-August-Universität Göttingen**

**I. Oswald, University of Strathclyde, Glasgow**

**H. Göbel, U. Göbel, LabXA, München**

**K. Janssens, University of Antwerp**

**R. Dinnebier, MPI Stuttgart**

**H. Ott, T. Stürzer, M. Ruf, B. Noll, S. Freisz, M. Benning, V. Smith, J. Kärcher, G. Bryant, R. Durst, Bruker AXS**

**B. Hasse, A. Kleine, U. Heidorn, F. Hertlein, C. Michaelsen, Incoatec**

# Thank You!

# Incoatec - Your Partner for X-Ray Optics and Microfocus Sources



Please visit our webpage for more information: [www.incoatec.de](http://www.incoatec.de)  
Or contact: [sales@incoatec.de](mailto:sales@incoatec.de)

Incoatec GmbH · Max-Planck-Str. 2 · 21502 Geesthacht · Germany ·  
Tel: +49(0)41 52 - 88 93 81 · [www.incoatec.de](http://www.incoatec.de)